

Supplementary Information:

Global upper ocean dissolved oxygen budget for constraining the biological carbon pump

Ryohei Yamaguchi^{1*}, Shinya Kouketsu^{1,2}, Naohiro Kosugi³, and Masao Ishii³

¹ *Research Institute for Global Change, Japan Agency for Marine-Earth Science and Technology, Yokosuka, Japan*

² *Advanced Institute for Marine Ecosystem Change (WPI-AIMEC), Japan Agency for Marine-Earth Science and Technology, Yokohama, Japan*

³ *Meteorological Research Institute, Japan Meteorological Agency, Tsukuba, Japan*

*Corresponding author: Ryohei Yamaguchi (ryamaguchi@jamstec.go.jp)

Contents

Note 1: Derivation of equations for upper ocean oxygen budget

Note 2: Model and parameters for estimating air-sea oxygen exchange and comparisons of estimates with previous studies

Note 3: Comparisons of estimated annual net community productions (ANCPs) with those from previous local studies

Figure 1: Three components of air-sea O₂ exchange and their drivers

Figure 2: Parameters for calculation of oxygen flux due to vertical diffusion

Figure 3: Distribution of sea surface dissolved oxygen data used in this study

Figure 4: Distribution of vertical profiles of dissolved oxygen used in this study

Figure 5: Comparisons of sea surface O₂ between BGC-Argo and GLODAP

Figure 6: Comparisons of air-sea O₂ fluxes with previous studies and different methods

Figure 7: Comparisons of ANCP with previous local and regional estimates

Table 1: Observational local estimates of ANCP in previous studies

Table 2: Methodological uncertainties in calculations of physical oxygen fluxes

Supplementary References

Supplementary Note 1 | Derivation of equations for upper ocean oxygen budget

Under conditions with negligible molecular diffusivities, an equation for the change in dissolved oxygen concentration ($[O_2]$, mol m⁻³) along a water parcel

$$\frac{D[O_2]}{Dt} = J, \quad (\text{S1})$$

and an equation for the thickness of the water parcel [h (m)]

$$\frac{\partial h}{\partial t} + \nabla \cdot (hv) = 0, \quad (\text{S2})$$

can be combined, yielding an equation for dissolved oxygen mass conservation,

$$\frac{\partial([O_2]h)}{\partial t} + \nabla \cdot ([O_2]hv) = hJ, \quad (\text{S3})$$

where J and \mathbf{v} indicate net dissolved oxygen change by biological production and respiration (mol m⁻³ s⁻¹) and velocity (m s⁻¹), respectively. Decomposing the variables into a large-scale component (denoted by an overbar, e.g., $\overline{[O_2]}$) and eddy components (denoted by a prime symbol, e.g., $[O_2]'$), and taking an average over the large-scale, equation (S3) becomes

$$\frac{\partial(\overline{[O_2]}\bar{h} + [O_2]'\bar{h}')}{\partial t} + \nabla \cdot (\overline{[O_2]}\bar{h}\mathbf{v} + \overline{[O_2]'}(h\mathbf{v})') = \bar{h}J. \quad (\text{S4})$$

Using the relationship $\bar{h}\mathbf{v} = (\bar{h}\bar{\mathbf{v}} + \bar{h}'\mathbf{v}')$, equation (S5) can be written as

$$\frac{\partial(\overline{[O_2]}\bar{h} + [O_2]'\bar{h}')}{\partial t} + \nabla \cdot \left(\overline{[O_2]}(\bar{h}\bar{\mathbf{v}} + \bar{h}'\mathbf{v}') \right) = -\nabla \cdot \overline{[O_2]'}(h\mathbf{v})' + \bar{h}J. \quad (\text{S5})$$

The same operation applied to equation (S3) yields

$$\frac{\partial \bar{h}}{\partial t} = -\nabla \cdot (\bar{h}\bar{\mathbf{v}} + \bar{h}'\mathbf{v}'). \quad (\text{S6})$$

Substituting equation (S6) into equation (S5) yields

$$\frac{\partial \overline{[O_2]}}{\partial t} + \frac{1}{\bar{h}} \frac{\partial \overline{[O_2]'}\bar{h}'}{\partial t} + \left(\bar{\mathbf{v}} + \frac{h'\mathbf{v}'}{\bar{h}} \right) \cdot \nabla \overline{[O_2]} = -\frac{1}{\bar{h}} \nabla \cdot \overline{[O_2]'}(h\mathbf{v})' + J. \quad (\text{S7})$$

With the assumption that the eddy components of the tracer and thickness are not correlated¹, the second term on the left side of equation (S7) becomes negligible:

$$\frac{\partial \overline{[O_2]}}{\partial t} + \left(\bar{\mathbf{v}} + \frac{h' \mathbf{v}'}{\bar{h}} \right) \cdot \nabla \overline{[O_2]} = -\frac{1}{\bar{h}} \nabla \cdot \overline{[O_2]'(h\mathbf{v})'} + J. \quad (\text{S8})$$

Parameterizing the first term on the right side of equation (S8) as Fickian diffusion with an eddy diffusion coefficient κ ($\text{m}^2 \text{s}^{-1}$), equation (S8) can be written in the form,

$$\frac{\partial [O_2]}{\partial t} = \nabla \cdot \kappa \nabla [O_2] - (\mathbf{v} + \mathbf{v}^*) \cdot \nabla [O_2] + J, \quad (\text{S9})$$

omitting the overbars for simplification and representing the bolus velocity $(h' \mathbf{v}' / \bar{h})$ as \mathbf{v}^* .

The eddy diffusion term consists of the horizontal component ($\nabla_h \cdot \kappa_h \nabla_h [O_2]$) and the vertical component ($\frac{\partial}{\partial z} \kappa_v \frac{\partial [O_2]}{\partial z}$). To obtain an equation for the upper ocean dissolved oxygen budget, equation (S9) is vertically integrated from the depth H ($z = -H$) to the sea surface ($z = 0$):

$$\begin{aligned} \frac{\partial}{\partial t} \int_{-H}^0 [O_2] dz &= \kappa_v(0) \frac{\partial [O_2]}{\partial z} \Big|_{z=0} - \kappa_v(-H) \frac{\partial [O_2]}{\partial z} \Big|_{z=-H} \\ &\quad + \int_{-H}^0 -(\mathbf{v} + \mathbf{v}^*) \cdot \nabla [O_2] dz + \int_{-H}^0 \nabla_h \cdot \kappa_h \nabla_h [O_2] dz + \int_{-H}^0 J dz. \end{aligned} \quad (\text{S10})$$

In the case where the target tracer is oxygen, the diffusion term at the sea surface corresponds to the air-sea exchange of oxygen. Therefore, an equation for the budget of the upper ocean oxygen ($O_{2\text{int}}$) can be written in the form

$$\frac{\partial O_{2\text{int}}}{\partial t} = F_{A-S} + F_{V\text{DIFF}} + F_{ADV} + F_{h\text{DIFF}} + F_{NCP}, \quad (\text{S11})$$

which indicates that changes in upper ocean oxygen result from air-sea oxygen exchange (F_{A-S}), vertical eddy diffusion of oxygen at the lower boundary depth H ($F_{V\text{DIFF}}$), advection of oxygen (F_{ADV}), horizontal eddy diffusion of oxygen ($F_{h\text{DIFF}}$), and net biological oxygen production (F_{NCP}).

Supplementary Note 2 | Model and parameters for estimating air-sea oxygen exchange and comparisons of estimates with previous studies

We used a model developed by a previous study² to estimate air-sea oxygen exchange from sea surface dissolved oxygen concentrations, temperature/salinity data, and sea surface wind speed products. This model is one of those developed to explicitly represent the role of bubbles in air-sea gas exchange, and was validated by comparison with direct field measurements of air-sea novel gas exchanges³. The model has also been used in several studies for estimating local net community production through oxygen mass balance⁴⁻⁶, and has been updated by tuning the parameters of the model to match observations^{7,8}.

In the model, the total air-sea oxygen exchange (F_{net}) is represented as the sum of the diffusive exchange at the air-sea interface (F_s) and two exchanges mediated by bubble processes in the vicinity of the air-sea interface (F_p and F_c)

$$F_{\text{net}} = F_s + \beta(F_p + F_c), \quad (\text{S12})$$

where β is a tuning parameter for adjusting to field observations ($\beta = 0.37$)⁸. These three components are written in the form

$$\begin{aligned} F_s &= k_s \left(\frac{P_{\text{slp}}}{P_{\text{atm}}} [\text{O}_2]_s^{\text{sat}} - [\text{O}_2]_s \right) \\ F_p &= k_p \left((1 + \Delta P) \frac{P_{\text{slp}}}{P_{\text{atm}}} [\text{O}_2]_s^{\text{sat}} - [\text{O}_2]_s \right) \\ F_c &= k_c \chi_{\text{atm}}^{\text{O}_2}, \end{aligned} \quad (\text{S13})$$

where $[\text{O}_2]_s$, $[\text{O}_2]_s^{\text{sat}}$, P_{slp} , P_{atm} , and $\chi_{\text{atm}}^{\text{O}_2}$ represent measured dissolved oxygen concentration at the surface; dissolved oxygen saturation concentration⁹ at the surface, calculated using measured sea surface temperature and salinity; sea level atmospheric pressure and one standard atmospheric pressure ($P_{\text{atm}} = 1013.25$ hPa); and the atmospheric mole fraction of oxygen ($\chi_{\text{atm}}^{\text{O}_2} = 0.21$), respectively.

The mass transfer coefficients (k_s , k_p , and k_c) and the fraction of supersaturation inside large bubbles (ΔP) are parameterized as functions of wind speed (adapted from Emerson and Bushinsky 2016):

$$\begin{aligned} k_s &= 1.04 \times 10^{-4} \times 1.3 \times u_*^a (S_c/660)^{-0.5} \\ k_p &= 5.5 \times (u_*^w)^{2.76} (S_c/660)^{-0.67} \\ k_c &= 5.56 \times (u_*^w)^{3.86} \\ \Delta P &= 1.52 \times (u_*^w)^{1.06}, \end{aligned} \tag{S14}$$

where u_*^a and u_*^w are the air-side and water-side friction velocities and S_c is the Schmidt number of oxygen at the sea surface temperature. The friction velocities are related by

$$u_*^w = \sqrt{\frac{\rho_a}{\rho_w}} u_*^a = \sqrt{\frac{\rho_a}{\rho_w}} \sqrt{C_d} U_{10}, \tag{S15}$$

where ρ_a , ρ_w , C_d and U_{10} represent air density, seawater density, drag coefficient at the air–water interface^{10,11}, and wind speed at 10 m height, respectively. We multiplied by the fraction of area not covered by sea ice ($1 - f_{ice}$) to obtain the net air–sea oxygen exchange (F_{A-S}):

$$F_{A-S} = F_{net} \times (1 - f_{ice}). \tag{S16}$$

The saturation oxygen concentration at the sea surface ($[O_2]_s^{sat}$) were calculated from the sea surface temperature and salinity obtained from each profile, using a skin layer temperature correction following a previous study¹². The skin layer temperatures at the position of each profile were obtained from ECMWF Reanalysis version 5, ERA5¹³. The sea surface saturation concentrations and the Schmidt number of oxygen were computed using a Python module¹⁴.

For obtaining daily wind speed at the location of individual ship/float profiles, we used satellite-based products (JOFURO3, Tomita et al. 2019; CCMPv2¹⁵) and atmospheric reanalysis products (JRA-55¹⁶; MERRA2¹⁷; ERA5¹³). For sea level pressure, we used ERA5. For sea ice concentrations, we used a satellite-derived daily product¹⁸. Wind speeds, sea level pressures and sea ice concentrations were spatially interpolated to get values at the locations and the times of individual ship/float profiles. With the interpolated these daily atmospheric variables, we calculated the three components of flux for individual profiles.

The flux values obtained from individual profiles were mapped, and the globally integrated air-sea exchange was estimated to be -206 ± 246 Tmol O₂ year⁻¹. The spread of the results mainly reflects the uncertainty from oxygen measurement and daily wind products. Our result, that the ocean has been outgassing in recent years, is consistent with several other studies confirming ocean deoxygenation^{19–21}. And, in the context of studies estimating the global carbon uptake in terrestrial and ocean regions based on observations of atmospheric oxygen and nitrogen, an increase in ocean outgassing due to an increase in ocean heat content is required, and its magnitude has been inferred at -53.9 ± 8.1 Tmol O₂ year⁻¹ (mean \pm SD of studies) since 1990^{22–26}.

The air-sea flux estimate presented in this study can be compared with the fluxes estimated over broad spatial extents by previous studies^{27–30}. These comparisons are illustrated in [Supplementary Figure 6](#). Gruber et al. (2001)²⁷ estimated global air-sea oxygen flux using an inversion method with a steady circulation field derived from a General Circulation Model (GCM) and observed ocean interior tracer data. While this method could be suffered by biases from the GCM circulation field, it does not require the strict parameterization of air-sea oxygen exchange at the surface, making it independent from our approach. Remarkable

differences in overall oxygen absorption/emission trends are seen in the Northern Hemisphere (temperate and northern North Pacific and North Atlantic), with this study showing a general trend of emission, whereas Gruber et al. (2001)²⁷ indicate an absorption (red and green bars in [Supplementary Fig. 6](#)). On the other hand, the fluxes for Earth System Models (ESM) summarized in Resplandy et al. (2015)³⁰ (mean of six CMIP5 models) and Li et al. (2020)²⁹ (mean of 10 CMIP5 models) shows the closer estimates to ours in some regions (temperate North Atlantic and North Pacific) with the large model spreads (red and orange/yellow bars in [Supplementary Fig. 6](#)). The discrepancy may be attributed to a number of factors, including differences in the analysis period, model biases in ESMs, assumptions made in the inversion, and incompleteness of the parameterizations for air-sea oxygen exchanges. Further validation, including studies employing additional independent methodologies, is required.

This study shares many of observational data used with Bushinsky et al. (2017)²⁸, and the air-sea oxygen fluxes were calculated in accordance with the majority of the methods employed in Bushinsky et al. (2017)²⁸. However, the flux calculation method differs in that we introduce a skin layer correction and the sea level pressure correction in the calculation of the sea surface oxygen saturation concentration. The modulations of the surface saturation by sea level pressure have more pronounced impact on the resultant flux in the Southern Ocean, where sea level pressure is lower than the standard pressure throughout the year ([Supplementary Fig. 1c](#)). With the surface pressure correction, the ocean uptake of oxygen in the Southern Ocean is considerably reduced (red and gray bars in [Supplementary Fig. 6](#)), while both are consistent in the case without the correction (blue and gray bars in [Supplementary Fig. 6](#)).

Prior to this study, Quay (2023)³¹ estimated the global ANCP based on the upper ocean oxygen and dissolved inorganic carbon (DIC) mass balance. Because Quay (2023)³¹ does not account for advection and horizontal diffusion fluxes in their oxygen budget calculation, described upper ocean dissolved oxygen mass balance is different from that of this study. In Quay (2023)³¹, an oxygen loss from the upper ocean due to the air-sea exchange was estimated ~ 800 Tmol O₂ year⁻¹ and an oxygen loss by vertical diffusion was reported as $\sim 10\%$ of the air-sea flux. These losses are balanced by the net biological oxygen production corresponding to an ANCP of 2.0 ± 0.8 mol C m⁻² year⁻¹. On the other hand, our results (but recalculated in the area aligned with Quay (2023)) demonstrated that the total ~ 590 Tmol O₂ year⁻¹ of oxygen loss, which is the sum of contributions from air-sea exchanges (~ 270 Tmol O₂ year⁻¹), diffusion (~ 190 Tmol O₂ year⁻¹), and advection (~ 130 Tmol O₂ year⁻¹), should be balanced by the net biological production corresponding an ANCP of 1.4 ± 0.5 mol C m⁻² year⁻¹. Despite the different overall descriptions of upper dissolved oxygen balance between the two studies, it is noteworthy that both ANCP estimates are consistent in terms of the overall characteristic of the spatial pattern, such as hemispheric and basin contrasts, and the two global estimates, including the range of uncertainty, overlap each other. It is likely because that the contributions from processes not considered in Quay (2023)³¹, such as advection and horizontal diffusion, affect the global integrated values of ANCP, yet have a limited impact on determining the basin contrast.

A comparison of the globally integrated air-sea oxygen fluxes calculated using similar approaches in both studies reveals that our estimate tends to be less release of oxygen from the ocean compared to the results of Quay (2023)³¹. This discrepancy might be attributed to two primary factors: (1) differences in the spatial and temporal resolution of the wind data used, and (2) the inclusion of a skin layer temperature correction. If one assumes that Quay

(2023)³¹ employed spatiotemporally more smoothed data (e.g., monthly climatological wind), it would likely yield different results from this study. As the parameterized equation of the air-sea oxygen flux is a nonlinear function of wind speed, the monthly average of fluxes calculated from daily wind speeds is not always identical to the flux calculated from monthly average wind speeds. Indeed, when fluxes were estimated using the same methodology, except for employing climatological monthly wind data, it was found that the underestimation of ocean oxygen uptake at high latitudes under strong winds resulted in a globally integrated flux with a 25% increase in the oxygen release.

The second reason could be the skin layer temperature correction employed in this study. Recent observational studies have suggested considering the skin effect when calculating the air-sea diffusion fluxes of CO₂ and oxygen^{12,32}. Generally, by using a slightly cooler skin layer temperature (temperature at the air-sea interface) instead of the bulk sea surface temperature (temperature at 15-m depth) to estimate the saturation concentration in diffusion flux calculations, the gas solubility increases, leading to a shift in the resultant flux towards more absorption. Indeed, the same calculation, excluding the skin layer temperature correction, yielded ~250 Tmol O₂ year⁻¹ increase in the ocean oxygen release on a global integrate basis. As previously reported¹², the differences are more pronounced in the subtropical regions (red and purple bars in [Supplementary Fig. 6](#)).

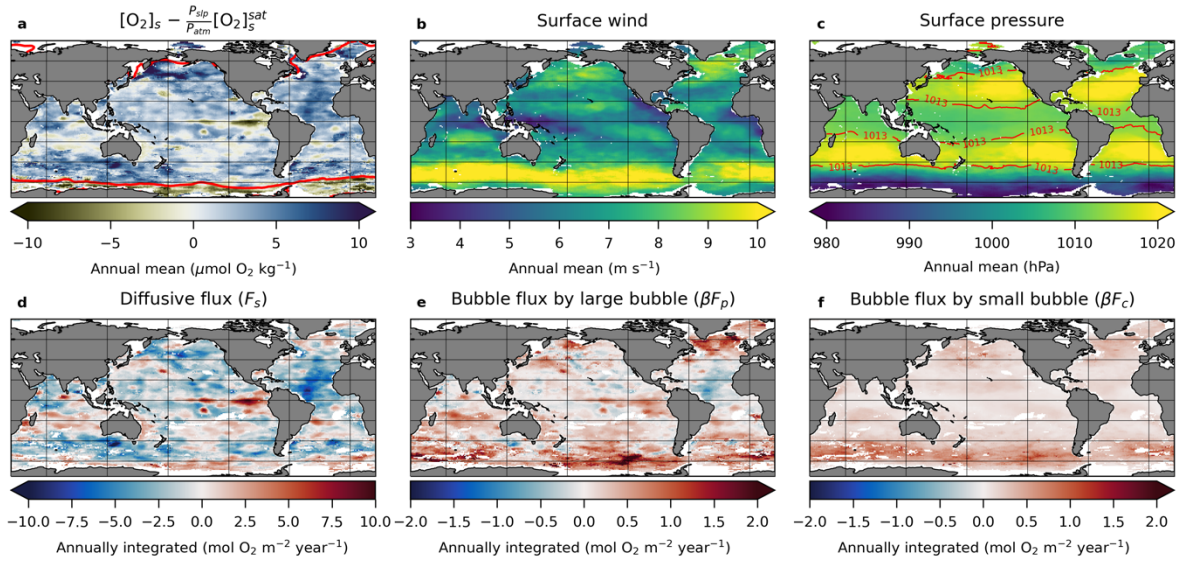
Supplementary Note 3 | Comparisons of estimated ANCPs with those from previous local studies

[Supplementary Figure 7](#) presents a comparison with local estimates from previous studies using various methodologies, which are summarized in [Supplementary Table 1](#). As seen in Figs. 4c–f, there is a general agreement in the overall spatial trends, with some exceptions (data outlined in the purple boxes in [Supplementary Figs. 7a](#) and [b](#)). Additionally, it was observed that the estimates from this study tend to be slightly smaller than those from previous studies. There are two main reasons why the estimates in this study appear smaller.

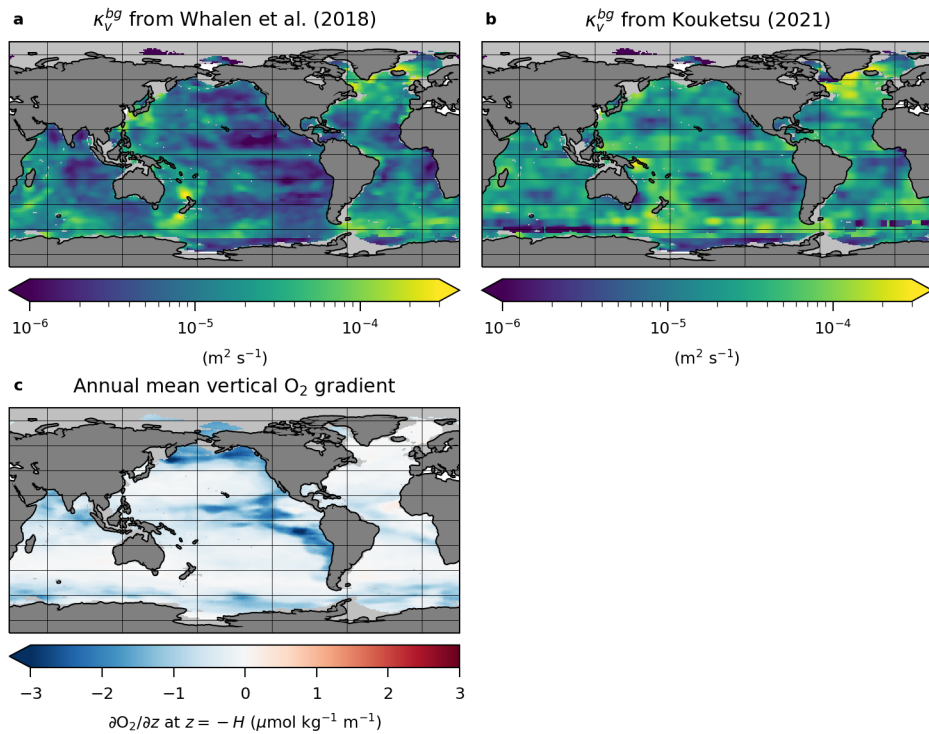
Firstly, it is important to note that some proportions of previous studies (~40% of N in [Supplementary Fig. 7a](#)) estimated ANCPs at depths shallower than the depth used in this study (depth H = the lower boundary of the upper ocean for the dissolved oxygen budget). These studies typically employed either temporally varying mixed layer depths (MLD) and euphotic layer depths (Z_{eu}), or fixed depths of 100 m and 200 m (c.f., [Supplementary Table 2](#)). In contrast, our approach utilizes the deeper of the annual maximum MLD or the annual maximum Z_{eu} . The NCP is determined as a balance between the net primary production (NPP) and the heterotrophic respiration (HR), that is $NCP = NPP - HR$. As NPP is more dominant within the euphotic zone and decreases with depth, where HR increases, NCP estimated from tracer budgets tends to decrease as the depth of H is defined more deeply³³. By categorizing previous estimates according to the definition of depth H and comparing them with our estimates, the discrepancies are less pronounced when compared to studies that employed the same definition of H .

Another contributing factor to the discrepancy is the inclusion of corrections for the skin layer temperature in calculations of air-sea oxygen flux. Incorporating the cooling effect of

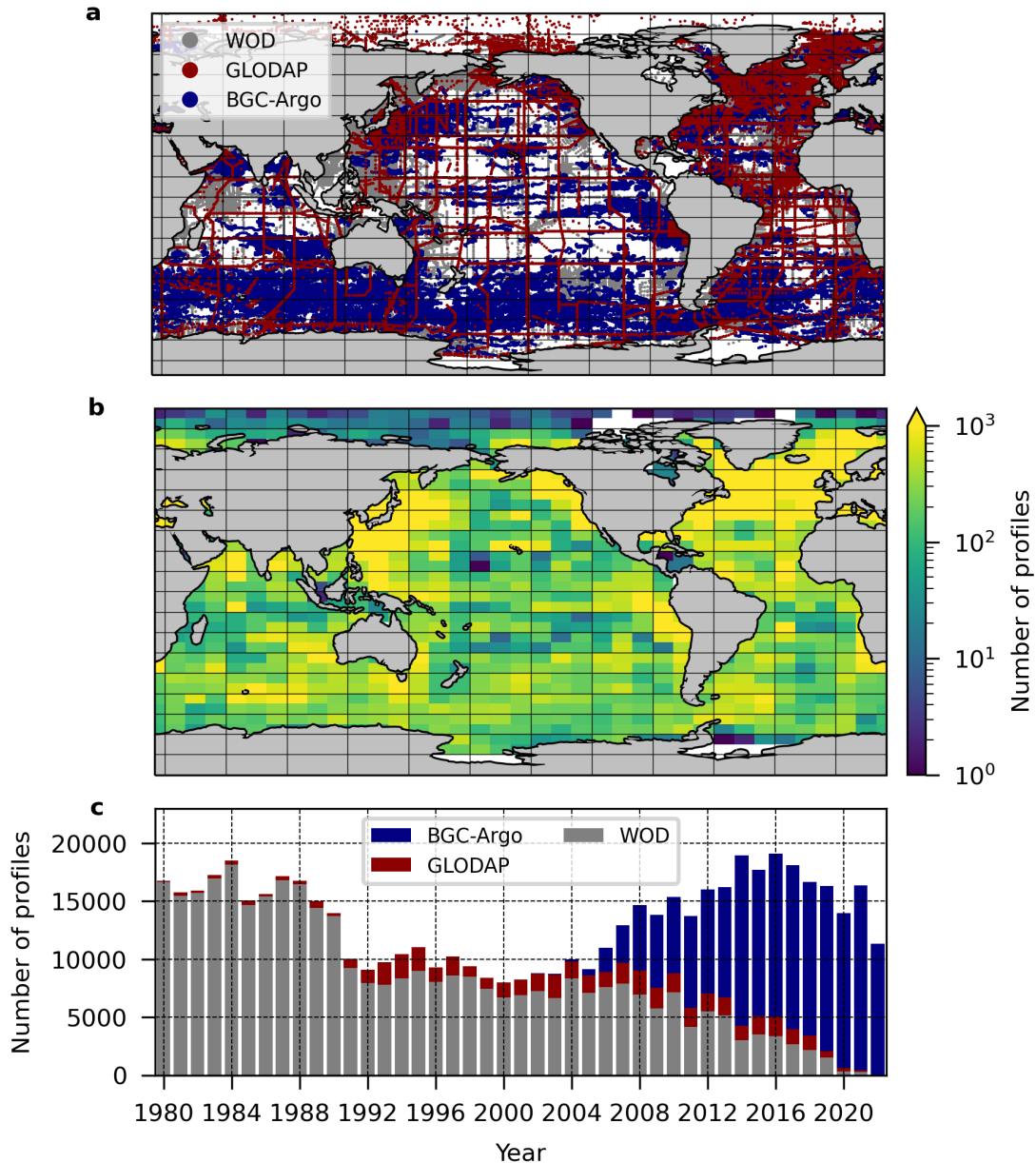
the surface skin layer into the calculation of oxygen saturation concentration results in a greater saturation concentration than in the case where this effect is not considered. This leads to an increase in ocean uptake of oxygen. Since, in the upper ocean dissolved oxygen budget equation applied in this study ([equation \[2\]](#)), an increase in sea surface oxygen uptake corresponds to a decrease in net biological oxygen production and hence ANCP, the skin layer temperature correction results in a smaller ANCP in this study than in previous studies. With the exception of a few recent studies^{12,34}, the majority of the previous studies included in the comparison here do not employ skin layer temperature correction.



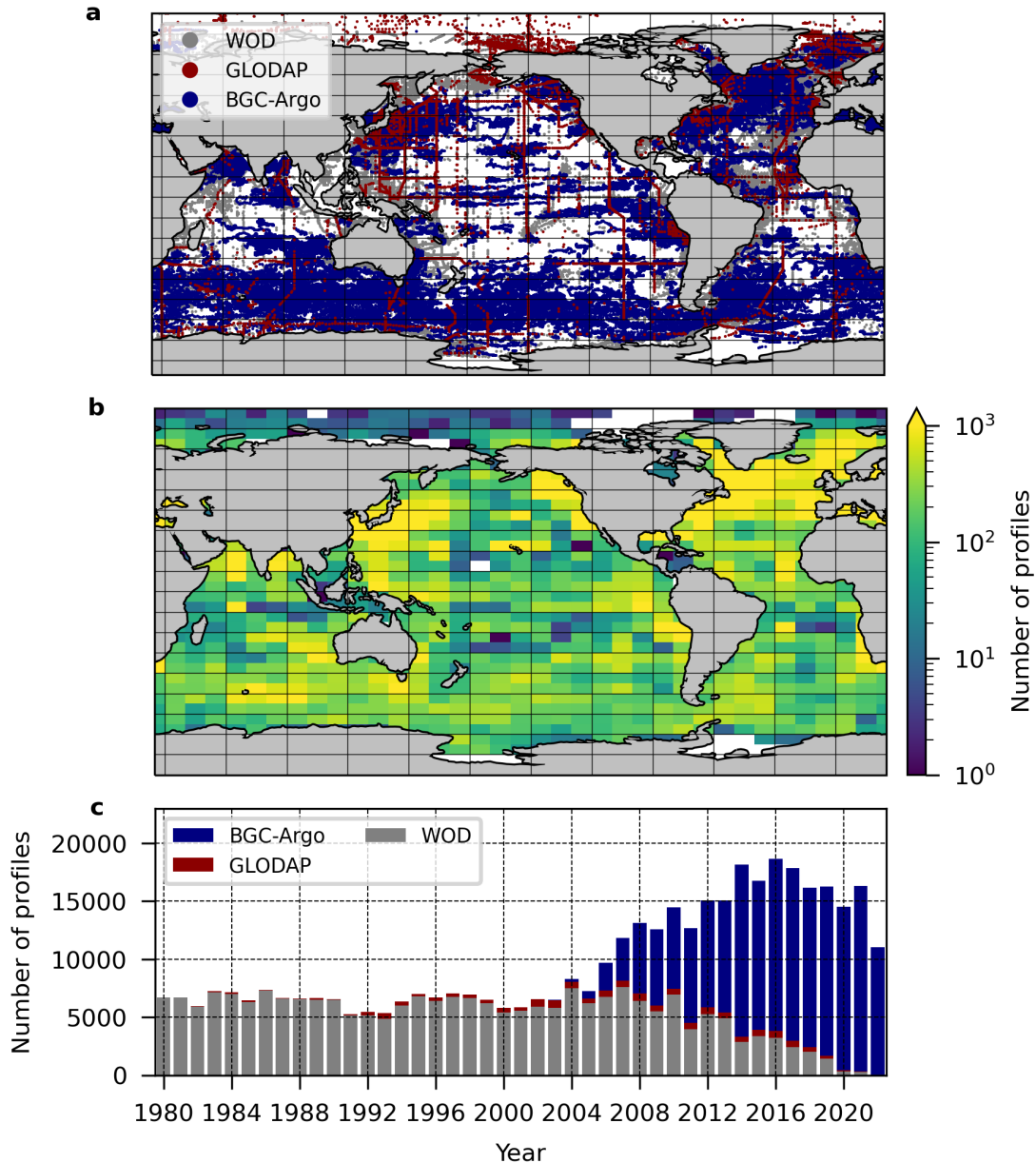
Supplementary Fig. 1 | Three components of air-sea O₂ exchange and their drivers. **a**, Annual mean differences between surface oxygen concentrations and saturation. Red lines indicate the annual maximum extent of sea ice (corresponding to sea ice fraction contours of 0.2). **b**, Annual mean wind speed at 10 m height. **c**, Annual mean sea level pressure. **d–f**, Annually integrated air-sea oxygen exchange through **(d)** diffusive flux (F_s), **(e)** bubble flux due to large bubbles that partially collapse (F_p), and **(f)** bubble flux due to small bubbles that completely collapse (F_c).



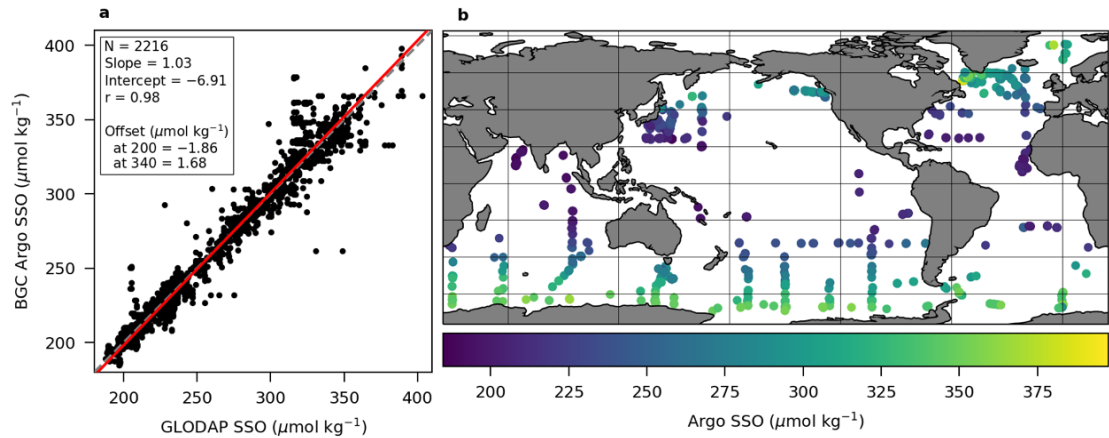
Supplementary Fig. 2 | Parameters for calculation of oxygen flux due to vertical diffusion. **a, b,** Background vertical diffusivity from Argo-based global three-dimensional vertical diffusivity products using fine-scale parameterization³⁵ and an inverse calculation for salinity on isopycnal surfaces³⁶. The background diffusivity was computed as the diffusivity value averaged vertically from the depth of $H + 100$ m to $H + 750$ m. Missing values on the data grid were replaced from another vertical diffusivity product based on tidal mixing parameterization³⁷. **c,** Annual mean vertical oxygen gradient at depth H . The vertical gradients were calculated from individual profiles and the profile values were then mapped. H was defined as the boundary depth of the upper ocean used in the calculation of the upper ocean oxygen budget, and was the deeper of the annual maximum mixed layer depth or the annual maximum euphotic layer depth.



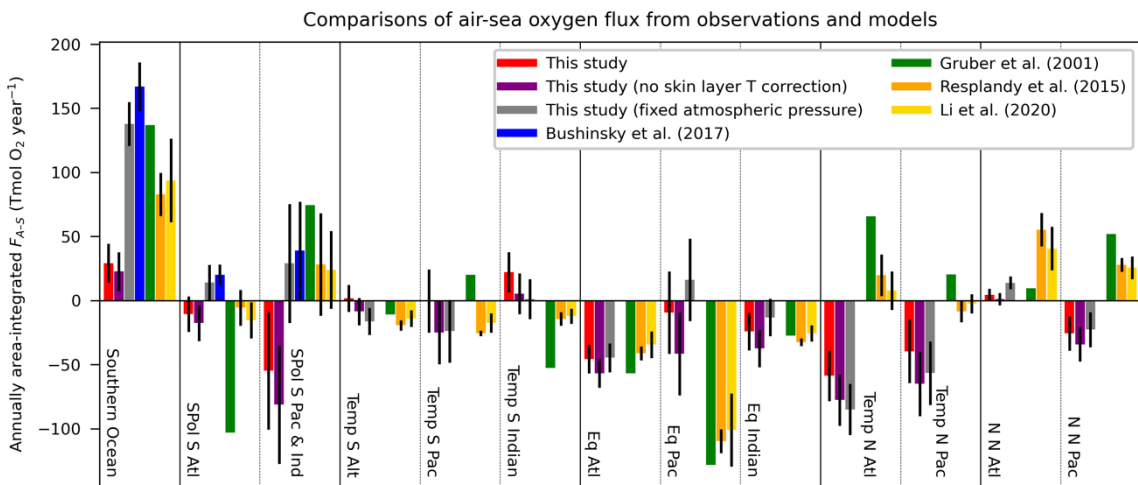
Supplementary Fig. 3 | Distribution of sea surface dissolved oxygen data used in this study. **a**, Spatial distribution of dissolved oxygen profiles from the World Ocean Database 2018 (WOD), the Global Ocean Data Analysis Project Version 2.2022 (GLODAP), and, the Biogeochemical-Argo data from the Global Data Assembly Centre (BGC-Argo). **b**, Number of profiles in 5° (latitude) $\times 10^{\circ}$ (longitude) boxes for the period 1980–2022. **c**, Global number of profiles per year.



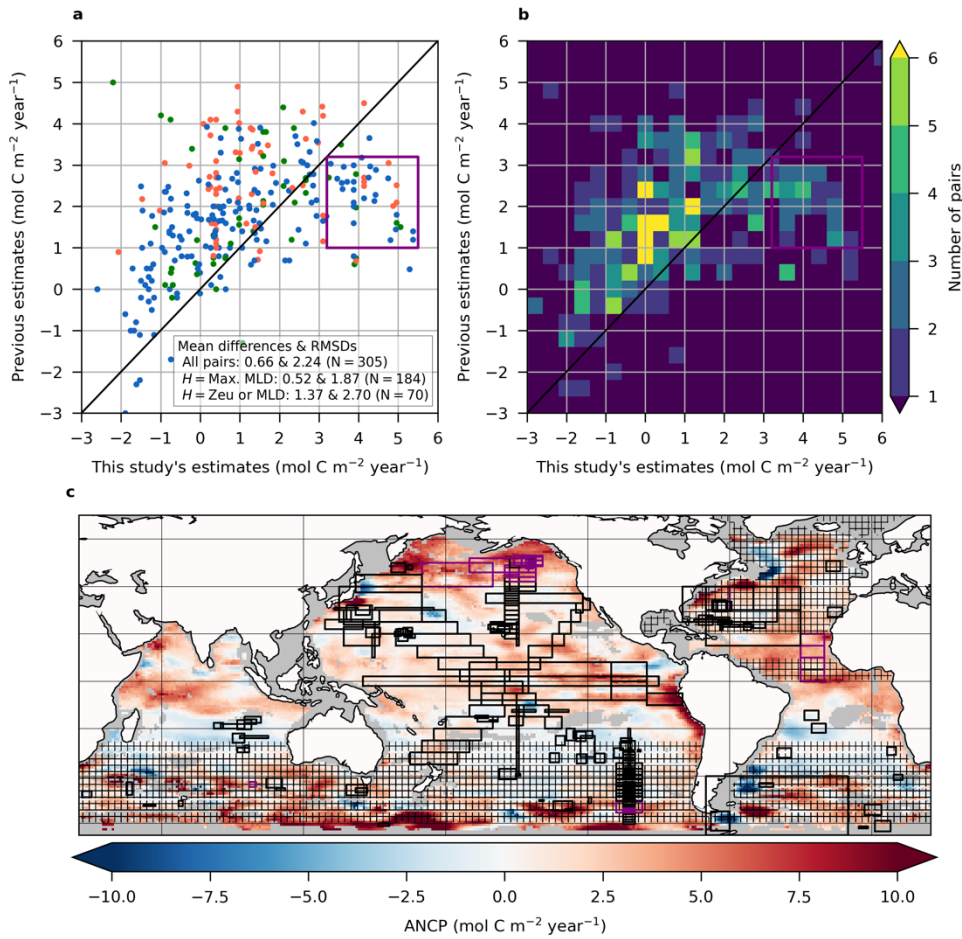
Supplementary Fig. 4 | Distribution of vertical profiles of dissolved oxygen used in this study. Same as Supplementary Fig. 3 but for the data used for the analyses that require not only surface values but also vertical profiles, such as estimations of vertical diffusion fluxes.



Supplementary Fig. 5 | Comparisons of sea surface O₂ between BGC-Argo and GLODAP. **a**, scatterplot for the comparison of sea surface oxygen (SSO) from the BGC-Argo and GLODAPv2.2022. Dots are crossover data that were matched to within ± 20 days, $\pm 0.5^\circ$ latitude, $\pm 0.5^\circ$ longitude, and ± 10 dbar. Model II regression and its statistics are shown as the red line and in the box. The gray dash line is 1:1 line. The offsets in the box are simple differences between the regression and 1:1 at given SSOs. **b**, Locations of the crossovers matched. Color indicates BGC-Argo SSO values at the crossovers.



Supplementary Fig. 6 | Comparisons of air-sea O_2 fluxes with previous studies and different methods. Based on the ocean area partitioning according to Gruber et al. (2001)²⁷ (their Figure 3), the air-sea oxygen fluxes estimated in this study were compared with model-based estimates (Gruber et al. 2001; Resplandy et al. 2015; Li et al. 2020)^{27,29,30} globally (green, orange, yellow bars, respectively) and observational estimates (Bushinsky et al. 2017)²⁸ only for the Southern Ocean (blue bars). For the fluxes from this study, results are also presented for calculations with sea level pressure fixed to standard atmospheric pressure (gray bars) and without skin temperature correction (purple bars). The vertical lines on the bars indicate their uncertainties where these are available.



Supplementary Fig. 7 | Comparisons of ANCP with previous local and regional estimates. **a**, Scatter plot for the comparisons of ANCP from this study and previous studies. The colors of dots represent the definitions of the depth by where ANCPs were estimated (depth H in case of this study); annual maximum MLD (blue), seasonally varying MLD or Z_{eu} (orange), and the others (green). **b**, two-dimensional histogram of **a**. Black lines in **a** and **b** are 1:1 line. **c**, Locations where the comparisons have been done. Black rectangles and hatches indicate regions where the individual previous ANCPs have been estimated. Purple rectangles show the locations of the data within the purple box in **a** and **b**. All data used in this figure and their references are summarized in [Table S1](#).

Supplementary Table 1 | Observational local estimates of annual net community production (ANCP) in previous studies

Basin	Latitudes		Longitudes		ANCP	SD/SE	Depth H	Methodology	Data length	Platform	Year of data	Reference	Notes for location and data source
Atlantic	48.50	48.75	343.80	343.80	4.30	1.30	Zeu (60m)	O ₂ budget	Full annual cycle	Seaglider	2012–2013	Binetti et al. (2020) ³⁸	PAP site
Atlantic	31.70	31.70	297.80	297.80	4.90	0.30	MLD	DIC/DI ¹³ C budget	Full annual cycle	Ship	1989–2000	Brix et al. (2006) ³⁹	BATS site
Atlantic	24.00	25.50	295.00	300.00	1.00	–	MMLD	O ₂ budget, Skin layer T correction	Full annual cycle	Float	2016–17	Emerson and Yang (2022) ³⁴	Float No.=9726
Atlantic	24.50	25.50	297.00	301.00	0.80	–	MMLD	O ₂ budget, Skin layer T correction	Full annual cycle	Float	2017–18	Emerson and Yang (2022) ³⁴	Float No.=9726
Atlantic	24.50	25.50	297.00	301.00	1.00	–	MMLD	O ₂ budget, Skin layer T correction	Full annual cycle	Float	2018–19	Emerson and Yang (2022) ³⁴	Float No.=9726
Atlantic	23.00	24.00	297.00	304.00	0.50	–	MMLD	O ₂ budget, Skin layer T correction	Full annual cycle	Float	2016–17	Emerson and Yang (2022) ³⁴	Float No.=9754
Atlantic	21.50	25.00	296.00	297.00	0.00	–	MMLD	O ₂ budget, Skin layer T correction	Full annual cycle	Float	2017–18	Emerson and Yang (2022) ³⁴	Float No.=9754
Atlantic	21.50	25.00	296.00	297.00	0.80	–	MMLD	O ₂ budget, Skin layer T correction	Full annual cycle	Float	2018–19	Emerson and Yang (2022) ³⁴	Float No.=9754
Atlantic	21.50	25.00	296.00	297.00	1.60	–	MMLD	O ₂ budget, Skin layer T correction	Full annual cycle	Float	2019–20	Emerson and Yang (2022) ³⁴	Float No.=9754
Atlantic	22.50	25.00	309.00	315.00	0.30	–	MMLD	O ₂ budget, Skin layer T correction	Full annual cycle	Float	2016–17	Emerson and Yang (2022) ³⁴	Float No.=9759
Atlantic	21.50	24.50	306.00	309.00	1.00	–	MMLD	O ₂ budget, Skin layer T correction	Full annual cycle	Float	2017–18	Emerson and Yang (2022) ³⁴	Float No.=9759
Atlantic	21.50	24.50	306.00	309.00	1.40	–	MMLD	O ₂ budget, Skin layer T correction	Full annual cycle	Float	2018–19	Emerson and Yang (2022) ³⁴	Float No.=9759
Atlantic	21.50	24.50	306.00	309.00	1.40	–	MMLD	O ₂ budget, Skin layer T correction	Full annual cycle	Float	2019–20	Emerson and Yang (2022) ³⁴	Float No.=9759
Atlantic	-16.36	-12.36	331.57	337.57	-0.10	–	MMLD	O ₂ budget, Skin layer T correction	Full annual cycle	Float	2019–20	Emerson and Yang (2022) ³⁴	Float No.=12691
Atlantic	-16.36	-12.36	331.57	337.57	0.40	–	MMLD	O ₂ budget, Skin layer T correction	Full annual cycle	Float	2020–21	Emerson and Yang (2022) ³⁴	Float No.=12691
Atlantic	-21.77	-17.77	334.66	340.66	0.50	–	MMLD	O ₂ budget, Skin layer T correction	Full annual cycle	Float	2019–20	Emerson and Yang (2022) ³⁴	Float No.=12632
Atlantic	-21.77	-17.77	334.66	340.66	1.10	–	MMLD	O ₂ budget, Skin layer T correction	Full annual cycle	Float	2020–21	Emerson and Yang (2022) ³⁴	Float No.=12632
Atlantic	-32.27	-28.27	319.99	325.99	0.10	–	MMLD	O ₂ budget, Skin layer T correction	Full annual cycle	Float	2020–21	Emerson and Yang (2022) ³⁴	Float No.=12785
Atlantic	32.10	32.10	295.50	295.50	0.92	0.50	MLD	DIC/DI ¹³ C budget	Full annual cycle	Ship	1883–1989	Gruber and Keeling (1999) ⁴⁰	Sta. S

Atlantic	31.50	31.50	295.84	295.84	2.30	0.90	MLD	DIC/DI ¹³ C budget	Full annual cycle	Ship	1991–1994	Gruber et al. (1998) ⁴¹	BATS site
Atlantic	31.50	31.50	295.84	295.84	3.40	0.80	MLD	DIC/DI ¹³ C budget	Full annual cycle	Ship	1983–2001	Gruber et al. (2002) ⁴²	BATS site
Atlantic	-65.00	-40.00	290.00	350.00	4.40	2.90	Fix (70dbar)	Subsurface respiration	Seasonal	Float	2015	Hennon et al. (2016) ⁴³	Drake Passage
Atlantic	25.00	40.00	280.00	320.00	3.90	2.30	Fix (70dbar)	Subsurface respiration	Seasonal	Float	2015	Hennon et al. (2016) ⁴³	Sargasso Sea
Atlantic	32.00	32.00	296.00	296.00	3.45	0.62	Zeu	O ₂ mass balance	Full annual cycle	Ship	1961–1978	Jenkins and Goldman (1985) ⁴⁴	Panulirus site (St. S)
Atlantic	-31.20	-27.80	6.50	10.20	0.00	–	Fix (200m)	NO ₃ drawdown	Seasonal	Float	2015	Johnson et al. (2017) ⁴⁵	Float No.=0037, WMO No.=5904475
Atlantic	-44.50	-42.90	312.40	318.50	3.40	–	Fix (200m)	NO ₃ drawdown	Seasonal	Float	2011–2012	Johnson et al. (2017) ⁴⁵	Float No.=5146, WMO No.=5901492
Atlantic	-41.70	-39.40	9.20	13.00	5.00	–	Fix (200m)	NO ₃ drawdown	Seasonal	Float	2012	Johnson et al. (2017) ⁴⁵	Float No.=6967, WMO No.=5903612
Atlantic	-61.30	-60.80	4.30	4.90	0.60	–	Fix (200m)	NO ₃ drawdown	Seasonal	Float	2015–2016	Johnson et al. (2017) ⁴⁵	Float No.=7652, WMO No.=5904467
Atlantic	-54.30	-54.00	0.00	1.10	2.10	–	Fix (200m)	NO ₃ drawdown	Seasonal	Float	2015–2016	Johnson et al. (2017) ⁴⁵	Float No.=9096, WMO No.=5904469
Atlantic	-62.00	-61.20	354.60	358.40	1.20	–	Fix (200m)	NO ₃ drawdown	Seasonal	Float	2015–2016	Johnson et al. (2017) ⁴⁵	Float No.=9125, WMO No.=5904397
Atlantic	-47.90	-42.60	45.20	47.50	4.10	–	Fix (200m)	NO ₃ drawdown	Seasonal	Float	2015–2016	Johnson et al. (2017) ⁴⁵	Float No.=9260, WMO No.=5904473
Atlantic	-63.00	-55.00	292.00	300.00	1.16	0.39	MLD	PO ₄ budget	Full annual cycle	Ship	2002–2011	Munro et al. (2015) ⁴⁶	Drake Passage Time-series
Atlantic	-63.00	-55.00	292.00	300.00	1.63	0.40	MLD	DIC budget	Full annual cycle	Ship	2002–2011	Munro et al. (2015) ⁴⁶	Drake Passage Time-series
Atlantic	29.16	29.16	344.50	344.50	3.30	1.00	MLD	DIC budget	Full annual cycle	Ship	1996–2000	Neuer et al. (2007) ⁴⁷	ESTOC
Atlantic	40.00	65.00	Basinwide	Basinwide	2.80	2.70	MLD	Steady annual air-sea O ₂ flux	Full annual cycle	Ship	1991–2005	Quay et al. (2012) ⁴⁸	CARINA
Atlantic	30.00	40.00	300.00	310.00	1.65	0.60	MMLD	DIC/DI ¹³ C mass balance	Snapshot	Ship	2011	Quay et al. (2020) ⁴⁹	GEOTRACES G10
Atlantic	30.00	40.00	290.00	300.00	2.57	1.00	MMLD	DIC/DI ¹³ C mass balance	Snapshot	Ship	2011	Quay et al. (2020) ⁴⁹	GEOTRACES G10
Atlantic	23.00	24.00	300.00	310.00	1.59	0.60	MMLD	DIC/DI ¹³ C mass balance	Snapshot	Ship	1998	Quay et al. (2020) ⁴⁹	WOCE Line A05
Atlantic	25.00	26.00	285.00	290.00	1.66	0.70	MMLD	DIC/DI ¹³ C mass balance	Snapshot	Ship	1998	Quay et al. (2020) ⁴⁹	WOCE Line A05
Atlantic	26.00	27.00	290.00	300.00	1.47	0.60	MMLD	DIC/DI ¹³ C mass balance	Snapshot	Ship	1998	Quay et al. (2020) ⁴⁹	WOCE Line A05

Atlantic	0.00	5.00	330.00	340.00	2.89	1.20	MMLD	DIC/DI ¹³ C mass balance	Snapshot	Ship	1993	Quay et al. (2020) ⁴⁹	WOCE Line A16
Atlantic	5.00	10.00	330.00	340.00	1.44	0.50	MMLD	DIC/DI ¹³ C mass balance	Snapshot	Ship	1993	Quay et al. (2020) ⁴⁹	WOCE Line A16
Atlantic	10.00	15.00	330.00	340.00	2.60	1.00	MMLD	DIC/DI ¹³ C mass balance	Snapshot	Ship	1993	Quay et al. (2020) ⁴⁹	WOCE Line A16
Atlantic	0.00	10.00	330.00	340.00	2.68	1.10	MMLD	DIC/DI ¹³ C mass balance	Snapshot	Ship	2003	Quay et al. (2020) ⁴⁹	WOCE Line A16
Atlantic	10.00	20.00	330.00	340.00	2.42	1.00	MMLD	DIC/DI ¹³ C mass balance	Snapshot	Ship	2003	Quay et al. (2020) ⁴⁹	WOCE Line A16
Atlantic	15.00	30.00	290.00	330.00	2.33	0.90	MMLD	DIC/DI ¹³ C mass balance	Snapshot	Ship	2003	Quay et al. (2020) ⁴⁹	WOCE Line A20/A22
Atlantic	30.00	40.00	290.00	330.00	2.78	1.10	MMLD	DIC/DI ¹³ C mass balance	Snapshot	Ship	2003	Quay et al. (2020) ⁴⁹	WOCE Line A20/A22
Atlantic	0.00	10.00	Basinwide	Basinwide	3.18	0.90	MMLD	O ₂ budget	Full annual cycle	Ship	1980–2006	Quay et al. (2020) ⁴⁹	CARINA
Atlantic	20.00	30.00	Basinwide	Basinwide	2.99	0.80	MMLD	O ₂ budget	Full annual cycle	Ship	1980–2006	Quay et al. (2020) ⁴⁹	CARINA
Atlantic	30.00	40.00	Basinwide	Basinwide	3.09	1.10	MMLD	O ₂ budget	Full annual cycle	Ship	1980–2006	Quay et al. (2020) ⁴⁹	CARINA
Atlantic	40.00	50.00	Basinwide	Basinwide	2.91	1.10	MMLD	O ₂ budget	Full annual cycle	Ship	1980–2006	Quay et al. (2020) ⁴⁹	CARINA
Atlantic	50.00	60.00	Basinwide	Basinwide	0.70	1.40	MMLD	O ₂ budget	Full annual cycle	Ship	1980–2006	Quay et al. (2020) ⁴⁹	CARINA
Atlantic	60.00	70.00	Basinwide	Basinwide	1.11	1.60	MMLD	O ₂ budget	Full annual cycle	Ship	1980–2006	Quay et al. (2020) ⁴⁹	CARINA
Atlantic	32.00	32.00	296.00	296.00	3.86	1.03	Zeu	O ₂ budget, Ar/He constraint	Full annual cycle	Ship	1985–1986	Spitzer and Jenkins (1989) ⁵⁰	BATS site
Atlantic	31.70	31.70	297.60	297.60	2.10	0.08	Zeu	AOUR based on ³ H/ ³ He TTD age	Full annual cycle	Ship	2003–2006	Stanley et al. (2012) ⁵¹	BATS site
Atlantic	31.70	31.70	297.80	297.80	4.30	0.90	Zeu	NO ₃ flux, ³ He constraint	Full annual cycle	Ship	2003–2006	Stanley et al. (2015) ⁵²	BATS site
Atlantic	25.83	25.83	289.93	289.93	1.60	0.20	MMLD	DIC/DI ¹³ C mass balance	Snapshot	Ship	1998	Yang et al. (2019) ⁶	WOCE Line A05
Global	-60.00	-55.00	Basinwide	Basinwide	1.98	0.85	Fix (200m)	NO ₃ drawdown	Seasonal	Float	2013–2018	Arteaga et al. (2019) ⁵³	
Global	-55.00	-50.00	Basinwide	Basinwide	2.63	0.87	Fix (200m)	NO ₃ drawdown	Seasonal	Float	2013–2018	Arteaga et al. (2019) ⁵³	
Global	-50.00	-45.00	Basinwide	Basinwide	1.56	1.40	Fix (200m)	NO ₃ drawdown	Seasonal	Float	2013–2018	Arteaga et al. (2019) ⁵³	
Global	-45.00	-40.00	Basinwide	Basinwide	2.04	0.61	Fix (200m)	NO ₃ drawdown	Seasonal	Float	2013–2018	Arteaga et al. (2019) ⁵³	

Global	-40.00	-35.00	Basinwide	Basinwide	0.61	1.03	Fix (200m)	NO ₃ drawdown	Seasonal	Float	2013–2018	Arteaga et al. (2019) ⁵³	
Global	-35.00	-30.00	Basinwide	Basinwide	0.36	0.16	Fix (200m)	NO ₃ drawdown	Seasonal	Float	2013–2018	Arteaga et al. (2019) ⁵³	
Global	-60.00	-55.00	Basinwide	Basinwide	0.75	1.54	Fix (100m)	Subsurface respiration	Seasonal	Float	2013–2018	Arteaga et al. (2019) ⁵³	
Global	-55.00	-50.00	Basinwide	Basinwide	2.69	0.56	Fix (100m)	Subsurface respiration	Seasonal	Float	2013–2018	Arteaga et al. (2019) ⁵³	
Global	-50.00	-45.00	Basinwide	Basinwide	1.72	1.34	Fix (100m)	Subsurface respiration	Seasonal	Float	2013–2018	Arteaga et al. (2019) ⁵³	
Global	-45.00	-40.00	Basinwide	Basinwide	2.13	0.78	Fix (100m)	Subsurface respiration	Seasonal	Float	2013–2018	Arteaga et al. (2019) ⁵³	
Global	-40.00	-35.00	Basinwide	Basinwide	1.31	1.10	Fix (100m)	Subsurface respiration	Seasonal	Float	2013–2018	Arteaga et al. (2019) ⁵³	
Global	-35.00	-30.00	Basinwide	Basinwide	1.19	0.59	Fix (100m)	Subsurface respiration	Seasonal	Float	2013–2018	Arteaga et al. (2019) ⁵³	
Global	-30.00	-25.00	Basinwide	Basinwide	0.63	0.00	Fix (200m)	NO ₃ drawdown	Seasonal	Float	2010–15	Johnson et al. (2017) ⁴⁵	Zonal mean of float results
Global	-40.00	-35.00	Basinwide	Basinwide	0.76	1.47	Fix (200m)	NO ₃ drawdown	Seasonal	Float	2010–15	Johnson et al. (2017) ⁴⁵	Zonal mean of float results
Global	-45.00	-40.00	Basinwide	Basinwide	3.22	1.00	Fix (200m)	NO ₃ drawdown	Seasonal	Float	2010–15	Johnson et al. (2017) ⁴⁵	Zonal mean of float results
Global	-50.00	-45.00	Basinwide	Basinwide	3.15	1.36	Fix (200m)	NO ₃ drawdown	Seasonal	Float	2010–15	Johnson et al. (2017) ⁴⁵	Zonal mean of float results
Global	-55.00	-50.00	Basinwide	Basinwide	2.33	1.35	Fix (200m)	NO ₃ drawdown	Seasonal	Float	2010–15	Johnson et al. (2017) ⁴⁵	Zonal mean of float results
Global	-60.00	-55.00	Basinwide	Basinwide	2.78	0.00	Fix (200m)	NO ₃ drawdown	Seasonal	Float	2010–15	Johnson et al. (2017) ⁴⁵	Zonal mean of float results
Global	-60.00	-55.00	Basinwide	Basinwide	0.69	2.33	MLD	NO ₃ budget	Full annual cycle	Ship	1980–90s	MacCready and Quay (2001) ⁵⁴	WOCE and US JGOFS
Global	-55.00	-50.00	Basinwide	Basinwide	3.64	2.52	MLD	NO ₃ budget	Full annual cycle	Ship	1980–90s	MacCready and Quay (2001) ⁵⁴	WOCE and US JGOFS
Global	-50.00	-45.00	Basinwide	Basinwide	4.02	1.76	MLD	NO ₃ budget	Full annual cycle	Ship	1980–90s	MacCready and Quay (2001) ⁵⁴	WOCE and US JGOFS
Global	-45.00	-40.00	Basinwide	Basinwide	2.08	1.15	MLD	NO ₃ budget	Full annual cycle	Ship	1980–90s	MacCready and Quay (2001) ⁵⁴	WOCE and US JGOFS
Global	-40.00	-35.00	Basinwide	Basinwide	0.81	0.42	MLD	NO ₃ budget	Full annual cycle	Ship	1980–90s	MacCready and Quay (2001) ⁵⁴	WOCE and US JGOFS
Indian	-17.50	-15.00	95.00	102.00	-2.30	–	MMLD	O ₂ budget, Skin layer T correction	Full annual cycle	Float	2016–17	Emerson and Yang (2022) ³⁴	Float No.=9763
Indian	-18.00	-16.00	95.00	100.00	-3.00	–	MMLD	O ₂ budget, Skin layer T correction	Full annual cycle	Float	2017–18	Emerson and Yang (2022) ³⁴	Float No.=9763

Indian	-18.00	-16.00	95.00	100.00	-0.60	-	MMLD	O ₂ budget, Skin layer T correction	Full annual cycle	Float	2018–19	Emerson and Yang (2022) ³⁴	Float No.=9763
Indian	-20.00	-18.00	85.00	95.00	-1.00	-	MMLD	O ₂ budget, Skin layer T correction	Full annual cycle	Float	2016–17	Emerson and Yang (2022) ³⁴	Float No.=9768
Indian	-20.00	-17.50	82.00	86.00	0.00	-	MMLD	O ₂ budget, Skin layer T correction	Full annual cycle	Float	2017–18	Emerson and Yang (2022) ³⁴	Float No.=9768
Indian	-20.00	-17.50	82.00	86.00	0.00	-	MMLD	O ₂ budget, Skin layer T correction	Full annual cycle	Float	2018–19	Emerson and Yang (2022) ³⁴	Float No.=9768
Indian	-26.00	-22.00	90.00	95.00	-1.00	-	MMLD	O ₂ budget, Skin layer T correction	Full annual cycle	Float	2016–17	Emerson and Yang (2022) ³⁴	Float No.=9737
Indian	-24.00	-23.00	93.00	105.00	-2.20	-	MMLD	O ₂ budget, Skin layer T correction	Full annual cycle	Float	2017–18	Emerson and Yang (2022) ³⁴	Float No.=9737
Indian	-24.00	-23.00	93.00	105.00	-1.10	-	MMLD	O ₂ budget, Skin layer T correction	Full annual cycle	Float	2018–19	Emerson and Yang (2022) ³⁴	Float No.=9737
Indian	-30.00	-27.00	95.00	97.00	-1.70	-	MMLD	O ₂ budget, Skin layer T correction	Full annual cycle	Float	2016–17	Emerson and Yang (2022) ³⁴	Float No.=9758
Indian	-30.00	-28.00	92.00	97.00	-0.20	-	MMLD	O ₂ budget, Skin layer T correction	Full annual cycle	Float	2017–18	Emerson and Yang (2022) ³⁴	Float No.=9758
Indian	-30.00	-28.00	92.00	97.00	-0.10	-	MMLD	O ₂ budget, Skin layer T correction	Full annual cycle	Float	2018–19	Emerson and Yang (2022) ³⁴	Float No.=9758
Indian	-30.00	-28.00	92.00	97.00	-0.10	-	MMLD	O ₂ budget, Skin layer T correction	Full annual cycle	Float	2019–20	Emerson and Yang (2022) ³⁴	Float No.=9758
Indian	-50.00	-30.00	Basinwide	Basinwide	3.80	1.10	Fix (70dbar)	Subsurface respiration	Seasonal	Float	2015	Hennon et al. (2016) ⁴³	Southern Indian Ocean
Indian	-48.90	-46.30	26.30	30.40	1.50	-	Fix (200m)	NO ₃ drawdown	Seasonal	Float	2015	Johnson et al. (2017) ⁴⁵	Float No.=0508, WMO No.=5904476
Indian	-52.60	-52.10	52.20	57.40	-1.30	-	Fix (200m)	NO ₃ drawdown	Seasonal	Float	2008–2009	Johnson et al. (2017) ⁴⁵	Float No.=5146, WMO No.=5901492
Indian	-52.60	-50.40	67.10	69.00	1.40	-	Fix (200m)	NO ₃ drawdown	Seasonal	Float	2009–2010	Johnson et al. (2017) ⁴⁵	Float No.=5146, WMO No.=5901492
Indian	-44.50	-42.50	97.00	99.80	2.70	-	Fix (200m)	NO ₃ drawdown	Seasonal	Float	2012–2013	Johnson et al. (2017) ⁴⁵	Float No.=7552, WMO No.=5903593
Indian	-42.90	-42.90	107.20	107.80	1.10	-	Fix (200m)	NO ₃ drawdown	Seasonal	Float	2013–2014	Johnson et al. (2017) ⁴⁵	Float No.=7552, WMO No.=5903593
Indian	-46.00	-45.10	108.40	112.10	3.10	-	Fix (200m)	NO ₃ drawdown	Seasonal	Float	2014–2015	Johnson et al. (2017) ⁴⁵	Float No.=7552, WMO No.=5903593
Indian	-18.35	-18.35	95.00	95.00	1.00	0.30	MMLD	DIC/DI ¹³ C mass balance	Snapshot	Ship	2007	Yang et al. (2019) ⁶	WOCE Line I09
Pacific	22.45	22.45	202.00	202.00	2.41	1.31	Zeu (150m)	²³⁴ Th derived flux, C mass balance	Full annual cycle	Ship	1999–2000	Benitez-Nelson et al. (2001) ⁵⁵	Sta. ALOHA
Pacific	22.45	22.45	202.00	202.00	2.82	0.35	MLD	DIC/DI ¹³ C budget	Full annual cycle	Ship	1988–2002	Brix et al. (2004) ⁵⁶	Sta. ALOHA

Pacific	22.45	22.45	202.00	202.00	3.10	0.30	MLD	DIC/DI ¹³ C budget	Full annual cycle	Ship	1989–2000	Brix et al. (2006) ³⁹	Sta. ALOHA
Pacific	50.00	50.00	215.00	215.00	2.10	–	MLD	O ₂ budget	Full annual cycle	Ship	1969–1978	Emerson (1987) ⁵⁷	Sta. P
Pacific	50.00	50.00	215.00	215.00	2.51	1.00	MLD	O ₂ budget, N ₂ constraint	Full annual cycle	Mooring	2007–2008	Emerson and Stump (2010) ⁵⁸	Sta. P
Pacific	19.40	22.10	160.00	164.00	0.70	–	MMLD	O ₂ budget, Skin layer T correction	Full annual cycle	Float	2015–16	Emerson and Yang (2022) ³⁴	Float No.=9294
Pacific	19.70	22.60	162.00	166.00	0.80	–	MMLD	O ₂ budget, Skin layer T correction	Full annual cycle	Float	2016–17	Emerson and Yang (2022) ³⁴	Float No.=9294
Pacific	19.30	21.30	163.00	165.50	0.40	–	MMLD	O ₂ budget, Skin layer T correction	Full annual cycle	Float	2017–18	Emerson and Yang (2022) ³⁴	Float No.=9294
Pacific	18.50	20.00	162.50	166.00	1.40	–	MMLD	O ₂ budget, Skin layer T correction	Full annual cycle	Float	2015–16	Emerson and Yang (2022) ³⁴	Float No.=9305
Pacific	18.30	20.00	164.50	167.00	1.00	–	MMLD	O ₂ budget, Skin layer T correction	Full annual cycle	Float	2016–17	Emerson and Yang (2022) ³⁴	Float No.=9305
Pacific	18.20	21.00	164.00	165.00	1.30	–	MMLD	O ₂ budget, Skin layer T correction	Full annual cycle	Float	2017–18	Emerson and Yang (2022) ³⁴	Float No.=9305
Pacific	17.00	20.00	160.00	164.00	1.50	–	MMLD	O ₂ budget, Skin layer T correction	Full annual cycle	Float	2015–16	Emerson and Yang (2022) ³⁴	Float No.=9306
Pacific	20.00	22.00	159.00	161.00	1.20	–	MMLD	O ₂ budget, Skin layer T correction	Full annual cycle	Float	2017–18	Emerson and Yang (2022) ³⁴	Float No.=9306
Pacific	20.00	22.00	159.00	161.00	0.80	–	MMLD	O ₂ budget, Skin layer T correction	Full annual cycle	Float	2017–18	Emerson and Yang (2022) ³⁴	Float No.=9306
Pacific	-17.00	-16.40	198.50	202.00	0.10	–	MMLD	O ₂ budget, Skin layer T correction	Full annual cycle	Float	2014–15	Emerson and Yang (2022) ³⁴	Float No.=8485
Pacific	-15.50	-14.50	192.50	198.00	0.60	–	MMLD	O ₂ budget, Skin layer T correction	Full annual cycle	Float	2016–17	Emerson and Yang (2022) ³⁴	Float No.=8485
Pacific	-34.28	-30.28	223.98	227.98	-1.10	–	MMLD	O ₂ budget, Skin layer T correction	Full annual cycle	Float	2019–20	Emerson and Yang (2022) ³⁴	Float No.=6963
Pacific	-34.28	-30.28	223.98	227.98	-0.20	–	MMLD	O ₂ budget, Skin layer T correction	Full annual cycle	Float	2020–21	Emerson and Yang (2022) ³⁴	Float No.=6963
Pacific	-34.74	-30.74	235.39	239.39	-0.80	–	MMLD	O ₂ budget, Skin layer T correction	Full annual cycle	Float	2019–20	Emerson and Yang (2022) ³⁴	Float No.=12374
Pacific	-34.43	-30.43	243.22	247.22	0.20	–	MMLD	O ₂ budget, Skin layer T correction	Full annual cycle	Float	2019–20	Emerson and Yang (2022) ³⁴	Float No.=12383
Pacific	-34.43	-30.43	243.22	247.22	-0.50	–	MMLD	O ₂ budget, Skin layer T correction	Full annual cycle	Float	2020–21	Emerson and Yang (2022) ³⁴	Float No.=12383
Pacific	-26.00	-24.00	254.00	258.50	-0.30	–	MMLD	O ₂ budget, Skin layer T correction	Full annual cycle	Float	2017–18	Emerson and Yang (2022) ³⁴	Float No.=12385
Pacific	-26.00	-24.00	254.00	258.50	0.00	–	MMLD	O ₂ budget, Skin layer T correction	Full annual cycle	Float	2018–19	Emerson and Yang (2022) ³⁴	Float No.=12385

Pacific	-26.00	-24.00	254.00	258.50	-0.30	-	MMLD	O ₂ budget, Skin layer T correction	Full annual cycle	Float	2019–20	Emerson and Yang (2022) ³⁴	Float No.=12385
Pacific	-26.00	-24.00	254.00	258.50	0.30	-	MMLD	O ₂ budget, Skin layer T correction	Full annual cycle	Float	2019–20	Emerson and Yang (2022) ³⁴	Float No.=12385
Pacific	-32.27	-28.27	251.04	255.04	0.20	-	MMLD	O ₂ budget, Skin layer T correction	Full annual cycle	Float	2019–20	Emerson and Yang (2022) ³⁴	Float No.=12770
Pacific	-32.27	-28.27	251.04	255.04	-0.20	-	MMLD	O ₂ budget, Skin layer T correction	Full annual cycle	Float	2020–21	Emerson and Yang (2022) ³⁴	Float No.=12770
Pacific	-25.32	-21.32	235.23	239.23	0.50	-	MMLD	O ₂ budget, Skin layer T correction	Full annual cycle	Float	2020–21	Emerson and Yang (2022) ³⁴	Float No.=18822
Pacific	-27.02	-23.02	226.42	230.42	0.00	-	MMLD	O ₂ budget, Skin layer T correction	Full annual cycle	Float	2020–21	Emerson and Yang (2022) ³⁴	Float No.=18827
Pacific	50.00	50.00	215.00	215.00	1.60	-	Fix (100m)	O ₂ budget, Ar/N ₂ constraint	Full annual cycle	Ship	1987–1989	Emerson et al. (1991) ⁵⁹	Sta. P
Pacific	22.45	22.45	202.00	202.00	1.00	0.70	Zeu (100m)	O ₂ /Ar/N ₂ budget	Full annual cycle	Ship	1990	Emerson et al. (1995) ⁶⁰	Sta. ALOHA
Pacific	22.45	22.45	202.00	202.00	1.60	0.90	Zeu	DIC/DI ¹³ C budget	Full annual cycle	Ship	1990–1995	Emerson et al. (1997) ⁶¹	Sta. ALOHA
Pacific	22.45	22.45	202.00	202.00	2.00	0.90	Zeu	Organic carbon budget	Full annual cycle	Ship	1990–1995	Emerson et al. (1997) ⁶¹	Sta. ALOHA
Pacific	22.45	22.45	202.00	202.00	2.70	1.70	Zeu	O ₂ budget, Ar/N ₂ constraint	Full annual cycle	Ship	1990–1995	Emerson et al. (1997) ⁶¹	Sta. ALOHA
Pacific	22.45	22.45	202.00	202.00	4.10	1.90	Zeu	O ₂ budget, O ₂ /N ₂ constraint	Full annual cycle	Ship	2005	Emerson et al. (2008) ⁶²	Sta. ALOHA
Pacific	22.75	22.75	202.00	202.00	4.10	1.90	Zeu	O ₂ budget, N ₂ constraint	Full annual cycle	Mooring	2005	Emerson et al. (2008) ⁶²	MOSEAN mooring
Pacific	47.50	51.50	214.00	217.00	2.01	1.00	MLD	DIC budget	Full annual cycle	Mooring	2007–2014	Fassbender et al. (2016) ⁶³	Sta. P
Pacific	26.00	32.00	138.00	149.00	7.00	3.00	MLD	DIC budget	Full annual cycle	Float	2007–2014	Fassbender et al. (2017) ⁶⁴	vicinity of KEO buoy
Pacific	22.45	22.45	202.00	202.00	1.45	0.41	Zeu (150m)	O ₂ /Ar mass balance	Full annual cycle	Ship	2013–2019	Ferrón et al. (2021) ⁶⁵	Sta. ALOHA
Pacific	22.45	22.45	202.00	202.00	1.1	0.50	Zeu (150m)	O ₂ budget, Ar/N ₂ /Ne constraint	Full annual cycle	Ship	2000–2001	Hamme and Emerson (2006) ⁶⁶	Sta. ALOHA
Pacific	24.00	24.00	132.00	142.00	0.75	0.15	Fix (100m)	DIC mass balance	Full annual cycle	Ship	2014–2019	Hashihama et al. (2021) ⁶⁷	
Pacific	49.00	53.00	209.00	221.00	1.40	0.60	MMLD	DIC budget	Full annual cycle	Float/Mooring	2009–2018	Haskell et al. (2020) ⁶⁸	Sta. P, WMO No.=5902128, 5903274, 5903405, 5903714, 5903891, 5904125
Pacific	49.00	53.00	209.00	221.00	1.20	0.50	MMLD	NO ₃ budget	Full annual cycle	Float/Mooring	2009–2018	Haskell et al. (2020) ⁶⁸	Sta. P, WMO No.=5902128, 5903274, 5903405, 5903714, 5903891, 5904125
Pacific	-8.00	8.00	190.00	265.00	2.52	2.26	MLD	O ₂ /Ar/ ¹⁷ Δ mass balance	Snapshot	Ship	2000–2001	Hendricks et al. (2005) ⁶⁹	

Pacific	25.00	40.00	135.00	170.00	3.80	1.80	Fix (70dbar)	Subsurface respiration	Seasonal	Float	2015	Hennon et al. (2016) ⁴³	Western Pacific
Pacific	49.50	50.70	215.30	217.50	4.50	1.50	Zeu	O ₂ budget	Full annual cycle	Float	2018–2020	Huang et al. (2022) ⁷⁰	WMO No.=5905988
Pacific	49.50	50.70	215.30	217.50	2.60	0.60	Zeu	NO ₃ budget	Full annual cycle	Float	2018–2020	Huang et al. (2022) ⁷⁰	WMO No.=5905988
Pacific	49.50	50.70	215.30	217.50	2.70	0.60	Zeu	DIC budget	Full annual cycle	Float	2018–2020	Huang et al. (2022) ⁷⁰	WMO No.=5905988
Pacific	49.50	50.70	215.30	217.50	2.50	0.80	Zeu	TA budget	Full annual cycle	Float	2018–2020	Huang et al. (2022) ⁷⁰	WMO No.=5905988
Pacific	24.00	30.00	137.00	152.00	4.00	1.58	MLD	DIC budget	Full annual cycle	Ship	1997	Ishii et al. (2001) ⁷¹	WOCE Line P09
Pacific	15.00	23.00	137.00	152.00	1.58	1.33	MLD	DIC budget	Full annual cycle	Ship	1997	Ishii et al. (2001) ⁷¹	WOCE Line P09
Pacific	31.70	31.70	297.80	297.80	7.64	2.37	Zeu	NO ₃ flux, ³ He constraint	Full annual cycle	Ship	1983–1988	Jenkins and Doney (2003) ⁷²	BATS site
Pacific	-29.10	-28.20	256.90	258.50	0.10	–	Fix (200m)	NO ₃ drawdown	Seasonal	Float	2013–2014	Johnson et al. (2017) ⁴⁵	Float No.=7553, WMO No.=5903755
Pacific	-29.50	-29.30	258.00	258.80	0.40	–	Fix (200m)	NO ₃ drawdown	Seasonal	Float	2014–2015	Johnson et al. (2017) ⁴⁵	Float No.=7553, WMO No.=5903755
Pacific	-29.70	-28.80	261.10	262.40	0.10	–	Fix (200m)	NO ₃ drawdown	Seasonal	Float	2015–2016	Johnson et al. (2017) ⁴⁵	Float No.=7553, WMO No.=5903755
Pacific	-61.00	-60.00	151.50	156.20	3.40	–	Fix (200m)	NO ₃ drawdown	Seasonal	Float	2014–2015	Johnson et al. (2017) ⁴⁵	Float No.=7620, WMO No.=5904104
Pacific	-46.20	-45.60	141.10	143.70	2.50	–	Fix (200m)	NO ₃ drawdown	Seasonal	Float	2015–2016	Johnson et al. (2017) ⁴⁵	Float No.=8514, WMO No.=5904467
Pacific	-52.60	-52.60	228.50	230.60	6.00	–	Fix (200m)	NO ₃ drawdown	Seasonal	Float	2014–2015	Johnson et al. (2017) ⁴⁵	Float No.=9031, WMO No.=5904396
Pacific	-51.60	-48.90	240.40	241.50	3.50	–	Fix (200m)	NO ₃ drawdown	Seasonal	Float	2015–2016	Johnson et al. (2017) ⁴⁵	Float No.=9031, WMO No.=5904396
Pacific	-50.60	-50.00	219.50	221.40	4.20	–	Fix (200m)	NO ₃ drawdown	Seasonal	Float	2014–2015	Johnson et al. (2017) ⁴⁵	Float No.=9095, WMO No.=5904188
Pacific	-54.50	-53.90	230.60	233.20	0.30	–	Fix (200m)	NO ₃ drawdown	Seasonal	Float	2015–2016	Johnson et al. (2017) ⁴⁵	Float No.=9095, WMO No.=5904188
Pacific	-40.00	-39.10	209.60	211.50	0.50	–	Fix (200m)	NO ₃ drawdown	Seasonal	Float	2014–2015	Johnson et al. (2017) ⁴⁵	Float No.=9254, WMO No.=5904395
Pacific	-39.30	-39.00	205.60	206.80	-0.20	–	Fix (200m)	NO ₃ drawdown	Seasonal	Float	2015–2016	Johnson et al. (2017) ⁴⁵	Float No.=9254, WMO No.=5904395
Pacific	-8.00	0.00	250.00	265.00	4.42	1.00	MLD	O ₂ /Ar budget	Snapshot	Ship	2003	Kaiser et al. (2005) ⁷³	along TAO buoys
Pacific	0.00	8.00	250.00	265.00	0.72	0.50	MLD	O ₂ /Ar budget	Snapshot	Ship	2003	Kaiser et al. (2005) ⁷³	along TAO buoys

Pacific	22.45	22.45	202.00	202.00	2.30	0.80	MLD	DIC/DI ¹³ C budget	Full annual cycle	Ship	1988–2002	Keeling et al. (2004) ⁷⁴	Sta. ALOHA
Pacific	22.45	22.45	202.00	202.00	1.20	2.80	MLD	DIC budget	Full annual cycle	Ship/ Mooring	2005–2021	Knor et al. (2023) ⁷⁵	Sta. ALOHA
Pacific	-50.00	-37.00	Basinwide	Basinwide	3.90	0.73	Fix (50m)	Subsurface respiration	Seasonal	Float	2007	Martz et al. (2008) ⁷⁶	WMO No.=3900333-4, 3900344-6, 3900348, 5900421, 5901043-52 5901054
Pacific	47.00	49.00	164.00	166.00	2.90	0.20	MLD	DIC mass balance	Seasonal	Ship	1997	Midorikawa et al. (2002) ⁷⁷	WOCE Line P13
Pacific	29.00	33.00	235.00	238.00	3.32	1.00	MLD	O ₂ /Ar mass balance	Full annual cycle	Ship	2005–2008	Munro et al. (2013) ⁷⁸	CalCOFI
Pacific	40.00	50.00	170.00	200.00	2.70	0.80	MMLD	O ₂ /Ar budget	Full annual cycle	Ship	2008–2012	Palevsky et al. (2016) ⁷⁹	M/V <i>OOCL Tianjin</i> and <i>Tokyo</i> tracks
Pacific	35.00	35.00	200.00	235.00	3.30	0.50	MMLD	O ₂ /Ar budget	Full annual cycle	Ship	2008–2012	Palevsky et al. (2016) ⁷⁹	M/V <i>OOCL Tianjin</i> and <i>Tokyo</i> tracks
Pacific	37.50	45.00	142.00	170.00	0.70	1.00	MMLD	O ₂ /Ar budget	Full annual cycle	Ship	2008–2012	Palevsky et al. (2016) ⁷⁹	M/V <i>OOCL Tianjin</i> and <i>Tokyo</i> tracks
Pacific	49.50	50.50	215.00	215.50	2.20	1.20	MMLD	O ₂ budget	Full annual cycle	Seaglider	2008–2010	Pelland et al. (2018) ⁸⁰	Sta. P
Pacific	48.50	52.50	212.00	221.00	1.50	0.60	Fix (35m)	NO ₃ budget	Full annual cycle	Float	2009–2014	Plant et al. (2016) ⁵	WMO No.=5902128, 5903274, 5903405, 5903714, 5903891, 5904125
Pacific	48.50	52.50	212.00	221.00	1.50	0.70	Fix (35m)	O ₂ budget	Full annual cycle	Float	2009–2014	Plant et al. (2016) ⁵	WMO No.=5902128, 5903274, 5903405, 5903714, 5903891, 5904125
Pacific	23.00	23.00	202.00	202.00	2.48	1.24	MLD	DIC/DI ¹³ C budget	Full annual cycle	Ship	1994–1999	Quay and Stutsman (2003) ⁸¹	Sta. ALOHA
Pacific	-30.00	-25.00	240.00	240.00	1.90	0.50	MLD	DIC/DI ¹³ C mass balance	Full annual cycle	Ship	2004–2005	Quay et al. (2009) ⁸²	M/V <i>Columbus Waikato</i> track
Pacific	-25.00	-20.00	231.00	234.50	2.18	0.52	MLD	DIC/DI ¹³ C mass balance	Full annual cycle	Ship	2004–2005	Quay et al. (2009) ⁸²	M/V <i>Columbus Waikato</i> track
Pacific	-20.00	-15.00	222.00	229.00	2.45	0.92	MLD	DIC/DI ¹³ C mass balance	Full annual cycle	Ship	2004–2005	Quay et al. (2009) ⁸²	M/V <i>Columbus Waikato</i> track
Pacific	-15.00	-10.00	213.00	223.50	3.05	0.59	MLD	DIC/DI ¹³ C mass balance	Full annual cycle	Ship	2004–2005	Quay et al. (2009) ⁸²	M/V <i>Columbus Waikato</i> track
Pacific	-10.00	-5.00	204.00	218.00	3.90	0.69	MLD	DIC/DI ¹³ C mass balance	Full annual cycle	Ship	2004–2005	Quay et al. (2009) ⁸²	M/V <i>Columbus Waikato</i> track
Pacific	-5.00	0.00	195.00	212.50	3.54	0.71	MLD	DIC/DI ¹³ C mass balance	Full annual cycle	Ship	2004–2005	Quay et al. (2009) ⁸²	M/V <i>Columbus Waikato</i> track
Pacific	0.00	5.00	186.00	207.00	2.84	0.74	MLD	DIC/DI ¹³ C mass balance	Full annual cycle	Ship	2004–2005	Quay et al. (2009) ⁸²	M/V <i>Columbus Waikato</i> track
Pacific	5.00	10.00	177.00	201.50	3.48	1.14	MLD	DIC/DI ¹³ C mass balance	Full annual cycle	Ship	2004–2005	Quay et al. (2009) ⁸²	M/V <i>Columbus Waikato</i> track
Pacific	10.00	15.00	168.00	196.00	3.29	0.76	MLD	DIC/DI ¹³ C mass balance	Full annual cycle	Ship	2004–2005	Quay et al. (2009) ⁸²	M/V <i>Columbus Waikato</i> track

Pacific	15.00	20.00	159.00	190.50	2.72	1.03	MLD	DIC/DI ¹³ C mass balance	Full annual cycle	Ship	2004–2005	Quay et al. (2009) ⁸²	M/V Columbus Waikato track
Pacific	20.00	25.00	150.00	185.00	2.42	1.63	MLD	DIC/DI ¹³ C mass balance	Full annual cycle	Ship	2004–2005	Quay et al. (2009) ⁸²	M/V Columbus Waikato track
Pacific	25.00	30.00	140.00	180.00	2.99	1.66	MLD	DIC/DI ¹³ C mass balance	Full annual cycle	Ship	2004–2005	Quay et al. (2009) ⁸²	M/V Columbus Waikato track
Pacific	23.00	23.00	202.00	202.00	3.72	1.00	MLD	O ₂ /Ar mass balance	Full annual cycle	Ship	2006–2008	Quay et al. (2010) ⁸³	Sta. ALOHA
Pacific	-13.00	-12.00	222.00	232.00	2.39	1.00	MMLD	DIC/DI ¹³ C mass balance	Snapshot	Ship	2015	Quay et al. (2020) ⁴⁹	GEOTRACES EPZT
Pacific	-13.00	-12.00	208.00	218.00	1.36	0.70	MMLD	DIC/DI ¹³ C mass balance	Snapshot	Ship	2015	Quay et al. (2020) ⁴⁹	GEOTRACES EPZT
Pacific	30.00	31.00	133.00	143.00	1.77	0.70	MMLD	DIC/DI ¹³ C mass balance	Snapshot	Ship	2004	Quay et al. (2020) ⁴⁹	WOCE Line P02
Pacific	30.00	31.00	150.00	175.00	1.66	0.60	MMLD	DIC/DI ¹³ C mass balance	Snapshot	Ship	2004	Quay et al. (2020) ⁴⁹	WOCE Line P02
Pacific	10.00	15.00	149.00	150.00	1.40	0.50	MMLD	DIC/DI ¹³ C mass balance	Snapshot	Ship	2005	Quay et al. (2020) ⁴⁹	WOCE Line P10
Pacific	15.00	20.00	149.00	150.00	2.61	1.10	MMLD	DIC/DI ¹³ C mass balance	Snapshot	Ship	2005	Quay et al. (2020) ⁴⁹	WOCE Line P10
Pacific	-20.00	-15.00	210.00	211.00	1.36	0.50	MMLD	DIC/DI ¹³ C mass balance	Snapshot	Ship	2006	Quay et al. (2020) ⁴⁹	WOCE Line P16N
Pacific	-15.00	-10.00	210.00	211.00	1.91	0.70	MMLD	DIC/DI ¹³ C mass balance	Snapshot	Ship	2006	Quay et al. (2020) ⁴⁹	WOCE Line P16N
Pacific	15.00	20.00	210.00	211.00	3.06	1.20	MMLD	DIC/DI ¹³ C mass balance	Snapshot	Ship	2006	Quay et al. (2020) ⁴⁹	WOCE Line P16N
Pacific	20.00	25.00	210.00	211.00	2.02	0.80	MMLD	DIC/DI ¹³ C mass balance	Snapshot	Ship	2006	Quay et al. (2020) ⁴⁹	WOCE Line P16N
Pacific	-40.00	-30.00	210.00	211.00	0.79	0.30	MMLD	DIC/DI ¹³ C mass balance	Snapshot	Ship	2005	Quay et al. (2020) ⁴⁹	WOCE Line P16S
Pacific	-30.00	-20.00	210.00	211.00	1.00	0.40	MMLD	DIC/DI ¹³ C mass balance	Snapshot	Ship	2005	Quay et al. (2020) ⁴⁹	WOCE Line P16S
Pacific	-40.00	-35.00	257.00	258.00	1.04	0.40	MMLD	DIC/DI ¹³ C mass balance	Snapshot	Ship	2007	Quay et al. (2020) ⁴⁹	WOCE Line P18
Pacific	-35.00	-30.00	257.00	258.00	0.60	0.20	MMLD	DIC/DI ¹³ C mass balance	Snapshot	Ship	2007	Quay et al. (2020) ⁴⁹	WOCE Line P18
Pacific	-30.00	-25.00	257.00	258.00	0.90	0.40	MMLD	DIC/DI ¹³ C mass balance	Snapshot	Ship	2007	Quay et al. (2020) ⁴⁹	WOCE Line P18
Pacific	-25.00	-20.00	257.00	258.00	1.92	0.80	MMLD	DIC/DI ¹³ C mass balance	Snapshot	Ship	2007	Quay et al. (2020) ⁴⁹	WOCE Line P18
Pacific	-35.00	-30.00	165.00	185.00	0.59	0.20	MMLD	DIC/DI ¹³ C mass balance	Full annual cycle	Ship	2004–2005	Quay et al. (2020) ⁴⁹	Volunteer Observing Ship

Pacific	-30.00	-25.00	170.00	190.00	0.70	0.30	MMLD	DIC/DI ¹³ C mass balance	Full annual cycle	Ship	2004–2005	Quay et al. (2020) ⁴⁹	Volunteer Observing Ship
Pacific	-25.00	-20.00	175.00	195.00	1.16	0.50	MMLD	DIC/DI ¹³ C mass balance	Full annual cycle	Ship	2004–2005	Quay et al. (2020) ⁴⁹	Volunteer Observing Ship
Pacific	-20.00	-15.00	180.00	200.00	1.30	0.50	MMLD	DIC/DI ¹³ C mass balance	Full annual cycle	Ship	2004–2005	Quay et al. (2020) ⁴⁹	Volunteer Observing Ship
Pacific	-15.00	-10.00	190.00	205.00	1.28	0.50	MMLD	DIC/DI ¹³ C mass balance	Full annual cycle	Ship	2004–2005	Quay et al. (2020) ⁴⁹	Volunteer Observing Ship
Pacific	-10.00	-5.00	195.00	210.00	2.57	1.00	MMLD	DIC/DI ¹³ C mass balance	Full annual cycle	Ship	2004–2005	Quay et al. (2020) ⁴⁹	Volunteer Observing Ship
Pacific	-5.00	5.00	205.00	215.00	3.00	1.20	MMLD	DIC/DI ¹³ C mass balance	Full annual cycle	Ship	2004–2005	Quay et al. (2020) ⁴⁹	Volunteer Observing Ship
Pacific	5.00	10.00	215.00	220.00	3.50	1.40	MMLD	DIC/DI ¹³ C mass balance	Full annual cycle	Ship	2004–2005	Quay et al. (2020) ⁴⁹	Volunteer Observing Ship
Pacific	10.00	15.00	215.00	225.00	3.70	1.50	MMLD	DIC/DI ¹³ C mass balance	Full annual cycle	Ship	2004–2005	Quay et al. (2020) ⁴⁹	Volunteer Observing Ship
Pacific	15.00	20.00	225.00	230.00	2.50	0.80	MMLD	DIC/DI ¹³ C mass balance	Full annual cycle	Ship	2004–2005	Quay et al. (2020) ⁴⁹	Volunteer Observing Ship
Pacific	20.00	25.00	228.00	233.00	1.96	0.80	MMLD	DIC/DI ¹³ C mass balance	Full annual cycle	Ship	2004–2005	Quay et al. (2020) ⁴⁹	Volunteer Observing Ship
Pacific	25.00	30.00	233.00	237.00	1.83	0.70	MMLD	DIC/DI ¹³ C mass balance	Full annual cycle	Ship	2004–2005	Quay et al. (2020) ⁴⁹	Volunteer Observing Ship
Pacific	30.00	35.00	238.00	241.00	2.10	0.80	MMLD	DIC/DI ¹³ C mass balance	Full annual cycle	Ship	2004–2005	Quay et al. (2020) ⁴⁹	Volunteer Observing Ship
Pacific	22.00	24.00	198.00	208.00	1.60	0.20	Zeu	O ₂ mass balance	Seasonal	Float	2002–2005	Riser and Johnson (2008) ⁸⁴	Float No.=0894, WMO No.=4900093
Pacific	-24.00	-21.00	234.00	242.00	0.90	0.40	Zeu	O ₂ mass balance	Seasonal	Float	2002–2005	Riser and Johnson (2008) ⁸⁴	Float No.=1326, WMO No.=5900420
Pacific	-47.00	-45.00	142.00	147.00	2.45	1.48	MLD	DIC drawdown	Seasonal	Mooring	2012	Shadwick et al. (2015) ⁸⁵	SOTS site
Pacific	30.00	30.00	208.00	208.00	2.20	0.50	Zeu	OUR based on CFC-11 age	Snapshot	Ship	1991	Sonnerup et al. (1999) ⁸⁶	WOCE Line P16
Pacific	19.99	19.99	208.00	208.00	2.91	0.48	MMLD	OUR based on CFCs/SF ₆ TTD age	Snapshot	Ship	2008	Sonnerup et al. (2013) ⁸⁶	STUD2008 cruise, WOCE Line P16N
Pacific	21.98	21.98	208.00	208.00	2.59	0.37	MMLD	OUR based on CFCs/SF ₆ TTD age	Snapshot	Ship	2008	Sonnerup et al. (2013) ⁸⁶	STUD2008 cruise, WOCE Line P16N
Pacific	25.96	25.96	208.00	208.00	2.70	0.31	MMLD	OUR based on CFCs/SF ₆ TTD age	Snapshot	Ship	2008	Sonnerup et al. (2013) ⁸⁶	STUD2008 cruise, WOCE Line P16N
Pacific	27.99	27.99	208.00	208.00	3.66	0.51	MMLD	OUR based on CFCs/SF ₆ TTD age	Snapshot	Ship	2008	Sonnerup et al. (2013) ⁸⁶	STUD2008 cruise, WOCE Line P16N
Pacific	29.98	29.98	208.00	208.00	3.87	0.49	MMLD	OUR based on CFCs/SF ₆ TTD age	Snapshot	Ship	2008	Sonnerup et al. (2013) ⁸⁶	STUD2008 cruise, WOCE Line P16N

Pacific	33.99	33.99	208.00	208.00	3.64	0.69	MMLD	OUR based on CFCs/SF ₆ TTD age	Snapshot	Ship	2008	Sonnerup et al. (2013) ⁸⁶	STUD2008 cruise, WOCE Line P16N
Pacific	35.98	35.98	208.00	208.00	3.92	0.49	MMLD	OUR based on CFCs/SF ₆ TTD age	Snapshot	Ship	2008	Sonnerup et al. (2013) ⁸⁶	STUD2008 cruise, WOCE Line P16N
Pacific	36.99	36.99	208.00	208.00	2.63	0.43	MMLD	OUR based on CFCs/SF ₆ TTD age	Snapshot	Ship	2008	Sonnerup et al. (2013) ⁸⁶	STUD2008 cruise, WOCE Line P16N
Pacific	38.00	38.00	208.00	208.00	2.53	0.68	MMLD	OUR based on CFCs/SF ₆ TTD age	Snapshot	Ship	2008	Sonnerup et al. (2013) ⁸⁶	STUD2008 cruise, WOCE Line P16N
Pacific	39.99	39.99	208.00	208.00	3.91	0.88	MMLD	OUR based on CFCs/SF ₆ TTD age	Snapshot	Ship	2008	Sonnerup et al. (2013) ⁸⁶	STUD2008 cruise, WOCE Line P16N
Pacific	41.98	41.98	208.00	208.00	4.01	0.63	MMLD	OUR based on CFCs/SF ₆ TTD age	Snapshot	Ship	2008	Sonnerup et al. (2013) ⁸⁶	STUD2008 cruise, WOCE Line P16N
Pacific	46.00	46.00	208.00	208.00	2.68	1.03	MMLD	OUR based on CFCs/SF ₆ TTD age	Snapshot	Ship	2008	Sonnerup et al. (2013) ⁸⁶	STUD2008 cruise, WOCE Line P16N
Pacific	46.98	46.98	208.00	208.00	2.13	0.57	MMLD	OUR based on CFCs/SF ₆ TTD age	Snapshot	Ship	2008	Sonnerup et al. (2013) ⁸⁶	STUD2008 cruise, WOCE Line P16N
Pacific	39.99	39.99	210.00	215.00	3.52	0.71	MMLD	OUR based on CFCs/SF ₆ TTD age	Snapshot	Ship	2008	Sonnerup et al. (2013) ⁸⁶	STUD2008 cruise
Pacific	39.99	39.99	210.00	215.00	2.33	0.23	MMLD	OUR based on CFCs/SF ₆ TTD age	Snapshot	Ship	2008	Sonnerup et al. (2013) ⁸⁶	STUD2008 cruise
Pacific	42.01	42.01	210.00	215.00	2.16	0.31	MMLD	OUR based on CFCs/SF ₆ TTD age	Snapshot	Ship	2008	Sonnerup et al. (2013) ⁸⁶	STUD2008 cruise
Pacific	41.98	41.98	210.00	215.00	1.77	0.17	MMLD	OUR based on CFCs/SF ₆ TTD age	Snapshot	Ship	2008	Sonnerup et al. (2013) ⁸⁶	STUD2008 cruise
Pacific	44.00	44.00	210.00	215.00	2.28	0.30	MMLD	OUR based on CFCs/SF ₆ TTD age	Snapshot	Ship	2008	Sonnerup et al. (2013) ⁸⁶	STUD2008 cruise
Pacific	46.00	46.00	210.00	215.00	1.45	0.25	MMLD	OUR based on CFCs/SF ₆ TTD age	Snapshot	Ship	2008	Sonnerup et al. (2013) ⁸⁶	STUD2008 cruise
Pacific	47.99	47.99	210.00	215.00	1.18	0.30	MMLD	OUR based on CFCs/SF ₆ TTD age	Snapshot	Ship	2008	Sonnerup et al. (2013) ⁸⁶	STUD2008 cruise
Pacific	50.01	50.01	210.00	215.00	0.48	0.15	MMLD	OUR based on CFCs/SF ₆ TTD age	Snapshot	Ship	2008	Sonnerup et al. (2013) ⁸⁶	STUD2008 cruise
Pacific	-60.26	-59.26	255.00	260.00	3.58	0.78	MMLD	OUR based on CFCs/SF ₆ TTD age	Snapshot	Ship	2007–2008	Sonnerup et al. (2015) ⁸⁷	WOCE Line P18
Pacific	-59.26	-58.27	255.00	260.00	2.32	0.32	MMLD	OUR based on CFCs/SF ₆ TTD age	Snapshot	Ship	2007–2008	Sonnerup et al. (2015) ⁸⁷	WOCE Line P18
Pacific	-58.27	-57.21	255.00	260.00	2.68	0.43	MMLD	OUR based on CFCs/SF ₆ TTD age	Snapshot	Ship	2007–2008	Sonnerup et al. (2015) ⁸⁷	WOCE Line P18
Pacific	-57.21	-56.09	255.00	260.00	3.32	0.48	MMLD	OUR based on CFCs/SF ₆ TTD age	Snapshot	Ship	2007–2008	Sonnerup et al. (2015) ⁸⁷	WOCE Line P18
Pacific	-56.09	-54.93	255.00	260.00	3.66	0.54	MMLD	OUR based on CFCs/SF ₆ TTD age	Snapshot	Ship	2007–2008	Sonnerup et al. (2015) ⁸⁷	WOCE Line P18

Pacific	-54.93	-54.04	255.00	260.00	2.97	0.55	MMLD	OUR based on CFCs/SF ₆ TTD age	Snapshot	Ship	2007–2008	Sonnerup et al. (2015) ⁸⁷	WOCE Line P18
Pacific	-54.04	-53.47	255.00	260.00	2.96	0.54	MMLD	OUR based on CFCs/SF ₆ TTD age	Snapshot	Ship	2007–2008	Sonnerup et al. (2015) ⁸⁷	WOCE Line P18
Pacific	-53.47	-52.88	255.00	260.00	3.03	0.54	MMLD	OUR based on CFCs/SF ₆ TTD age	Snapshot	Ship	2007–2008	Sonnerup et al. (2015) ⁸⁷	WOCE Line P18
Pacific	-52.88	-52.00	255.00	260.00	2.78	0.42	MMLD	OUR based on CFCs/SF ₆ TTD age	Snapshot	Ship	2007–2008	Sonnerup et al. (2015) ⁸⁷	WOCE Line P18
Pacific	-52.00	-50.84	255.00	260.00	2.04	0.38	MMLD	OUR based on CFCs/SF ₆ TTD age	Snapshot	Ship	2007–2008	Sonnerup et al. (2015) ⁸⁷	WOCE Line P18
Pacific	-50.84	-49.98	255.00	260.00	2.41	0.36	MMLD	OUR based on CFCs/SF ₆ TTD age	Snapshot	Ship	2007–2008	Sonnerup et al. (2015) ⁸⁷	WOCE Line P18
Pacific	-49.98	-49.32	255.00	260.00	1.83	0.36	MMLD	OUR based on CFCs/SF ₆ TTD age	Snapshot	Ship	2007–2008	Sonnerup et al. (2015) ⁸⁷	WOCE Line P18
Pacific	-49.32	-48.44	255.00	260.00	2.36	0.39	MMLD	OUR based on CFCs/SF ₆ TTD age	Snapshot	Ship	2007–2008	Sonnerup et al. (2015) ⁸⁷	WOCE Line P18
Pacific	-48.44	-47.64	255.00	260.00	2.48	0.40	MMLD	OUR based on CFCs/SF ₆ TTD age	Snapshot	Ship	2007–2008	Sonnerup et al. (2015) ⁸⁷	WOCE Line P18
Pacific	-47.64	-47.07	255.00	260.00	1.90	0.46	MMLD	OUR based on CFCs/SF ₆ TTD age	Snapshot	Ship	2007–2008	Sonnerup et al. (2015) ⁸⁷	WOCE Line P18
Pacific	-47.07	-46.49	255.00	260.00	2.49	0.45	MMLD	OUR based on CFCs/SF ₆ TTD age	Snapshot	Ship	2007–2008	Sonnerup et al. (2015) ⁸⁷	WOCE Line P18
Pacific	-46.49	-45.90	255.00	260.00	2.19	0.33	MMLD	OUR based on CFCs/SF ₆ TTD age	Snapshot	Ship	2007–2008	Sonnerup et al. (2015) ⁸⁷	WOCE Line P18
Pacific	-45.90	-45.30	255.00	260.00	2.36	0.29	MMLD	OUR based on CFCs/SF ₆ TTD age	Snapshot	Ship	2007–2008	Sonnerup et al. (2015) ⁸⁷	WOCE Line P18
Pacific	-45.30	-44.73	255.00	260.00	1.80	0.22	MMLD	OUR based on CFCs/SF ₆ TTD age	Snapshot	Ship	2007–2008	Sonnerup et al. (2015) ⁸⁷	WOCE Line P18
Pacific	-44.73	-44.15	255.00	260.00	1.85	0.19	MMLD	OUR based on CFCs/SF ₆ TTD age	Snapshot	Ship	2007–2008	Sonnerup et al. (2015) ⁸⁷	WOCE Line P18
Pacific	-44.15	-43.27	255.00	260.00	2.14	0.25	MMLD	OUR based on CFCs/SF ₆ TTD age	Snapshot	Ship	2007–2008	Sonnerup et al. (2015) ⁸⁷	WOCE Line P18
Pacific	-43.27	-42.39	255.00	260.00	1.95	0.10	MMLD	OUR based on CFCs/SF ₆ TTD age	Snapshot	Ship	2007–2008	Sonnerup et al. (2015) ⁸⁷	WOCE Line P18
Pacific	-42.39	-41.51	255.00	260.00	1.88	0.21	MMLD	OUR based on CFCs/SF ₆ TTD age	Snapshot	Ship	2007–2008	Sonnerup et al. (2015) ⁸⁷	WOCE Line P18
Pacific	-41.51	-40.63	255.00	260.00	1.45	0.11	MMLD	OUR based on CFCs/SF ₆ TTD age	Snapshot	Ship	2007–2008	Sonnerup et al. (2015) ⁸⁷	WOCE Line P18
Pacific	-40.63	-40.05	255.00	260.00	2.00	0.25	MMLD	OUR based on CFCs/SF ₆ TTD age	Snapshot	Ship	2007–2008	Sonnerup et al. (2015) ⁸⁷	WOCE Line P18
Pacific	-40.05	-39.48	255.00	260.00	1.96	0.31	MMLD	OUR based on CFCs/SF ₆ TTD age	Snapshot	Ship	2007–2008	Sonnerup et al. (2015) ⁸⁷	WOCE Line P18

Pacific	-39.48	-38.88	255.00	260.00	1.65	0.13	MMLD	OUR based on CFCs/SF ₆ TTD age	Snapshot	Ship	2007–2008	Sonnerup et al. (2015) ⁸⁷	WOCE Line P18
Pacific	-38.88	-38.29	255.00	260.00	1.68	0.24	MMLD	OUR based on CFCs/SF ₆ TTD age	Snapshot	Ship	2007–2008	Sonnerup et al. (2015) ⁸⁷	WOCE Line P18
Pacific	-38.29	-37.43	255.00	260.00	1.69	0.16	MMLD	OUR based on CFCs/SF ₆ TTD age	Snapshot	Ship	2007–2008	Sonnerup et al. (2015) ⁸⁷	WOCE Line P18
Pacific	-37.43	-36.56	255.00	260.00	1.69	0.41	MMLD	OUR based on CFCs/SF ₆ TTD age	Snapshot	Ship	2007–2008	Sonnerup et al. (2015) ⁸⁷	WOCE Line P18
Pacific	-36.56	-35.68	255.00	260.00	1.72	0.17	MMLD	OUR based on CFCs/SF ₆ TTD age	Snapshot	Ship	2007–2008	Sonnerup et al. (2015) ⁸⁷	WOCE Line P18
Pacific	-35.68	-34.51	255.00	260.00	1.27	0.03	MMLD	OUR based on CFCs/SF ₆ TTD age	Snapshot	Ship	2007–2008	Sonnerup et al. (2015) ⁸⁷	WOCE Line P18
Pacific	-34.51	-33.35	255.00	260.00	1.79	0.10	MMLD	OUR based on CFCs/SF ₆ TTD age	Snapshot	Ship	2007–2008	Sonnerup et al. (2015) ⁸⁷	WOCE Line P18
Pacific	-33.35	-32.18	255.00	260.00	2.02	0.22	MMLD	OUR based on CFCs/SF ₆ TTD age	Snapshot	Ship	2007–2008	Sonnerup et al. (2015) ⁸⁷	WOCE Line P18
Pacific	-32.18	-31.02	255.00	260.00	1.77	0.16	MMLD	OUR based on CFCs/SF ₆ TTD age	Snapshot	Ship	2007–2008	Sonnerup et al. (2015) ⁸⁷	WOCE Line P18
Pacific	-31.02	-29.87	255.00	260.00	1.85	0.19	MMLD	OUR based on CFCs/SF ₆ TTD age	Snapshot	Ship	2007–2008	Sonnerup et al. (2015) ⁸⁷	WOCE Line P18
Pacific	-2.00	2.00	145.00	190.00	1.50	0.20	MLD	O ₂ /Ar mass balance	Snapshot	Ship	2006	Stanley et al. (2010) ⁸⁸	
Pacific	48.00	48.00	160.00	160.00	1.49	0.42	MMLD	DIC budget	Full annual cycle	Ship	2004–2013	Wakita et al. (2016) ⁸⁹	Sta. K2
Pacific	30.00	30.00	145.00	145.00	2.81	0.53	MMLD	DIC budget	Full annual cycle	Ship	2004–2013	Wakita et al. (2016) ⁸⁹	Sta. S1
Pacific	46.00	52.00	190.00	215.00	3.05	—	MLD	NO ₃ drawdown	Seasonal	Ship	1995–1997	Wong et al. (2002) ⁹⁰	M/V <i>Skaugran</i> , Alaska Gyre
Pacific	22.00	24.00	202.00	207.00	2.00	—	MMLD	O ₂ budget	Full annual cycle	Float	2014–15	Yang et al. (2017) ⁷	Float No.=8497
Pacific	49.00	51.00	215.00	221.00	2.00	—	MMLD	DIC budget	Full annual cycle	Mooring	2012–13	Yang et al. (2018) ⁹¹	Sta. P
Pacific	49.00	51.00	215.00	221.00	2.10	—	MMLD	DIC budget	Full annual cycle	Mooring	2013–14	Yang et al. (2018) ⁹¹	Sta. P
Pacific	49.00	51.00	215.00	221.00	2.60	—	MMLD	DIC budget	Full annual cycle	Mooring	2014–15	Yang et al. (2018) ⁹¹	Sta. P
Pacific	49.00	51.00	215.00	221.00	3.00	—	MMLD	DIC budget	Full annual cycle	Mooring	2015–16	Yang et al. (2018) ⁹¹	Sta. P
Pacific	49.00	51.00	215.00	221.00	2.40	0.60	MMLD	O ₂ Budget	Full annual cycle	Float	2012–13	Yang et al. (2018) ⁹¹	Float No.=8397, WMO No.=5903743
Pacific	49.00	51.00	215.00	221.00	0.80	0.40	MMLD	O ₂ Budget	Full annual cycle	Float	2013–14	Yang et al. (2018) ⁹¹	Float No.=8397, WMO No.=5903743

Pacific	49.00	51.00	215.00	221.00	1.60	0.40	MMLD	O ₂ Budget	Full annual cycle	Float	2015–16	Yang et al. (2018) ⁹¹	Float No.=8397, WMO No.=5903743
Pacific	20.50	23.30	202.00	207.00	2.00	–	MMLD	O ₂ budget	Full annual cycle	Float	2013–14	Yang et al. (2019) ⁶	Float No.=8497
Pacific	-17.00	-15.00	193.50	202.00	0.50	–	MMLD	O ₂ budget	Full annual cycle	Float	2015–16	Yang et al. (2019) ⁶	Float No.=8485
Pacific	22.40	22.40	208.00	208.00	2.10	0.20	MMLD	DIC/DI ¹³ C mass balance	Snapshot	Ship	2006	Yang et al. (2019) ⁶	WOCE Line P16N
Pacific	20.60	20.60	149.30	149.30	2.40	0.40	MMLD	DIC/DI ¹³ C mass balance	Snapshot	Ship	2005	Yang et al. (2019) ⁶	WOCE Line P10
Pacific	-16.71	-16.71	209.77	209.77	1.20	0.10	MMLD	DIC/DI ¹³ C mass balance	Snapshot	Ship	2005	Yang et al. (2019) ⁶	WOCE Line P16S
Pacific	-27.06	-27.06	257.00	257.00	1.00	0.10	MMLD	DIC/DI ¹³ C mass balance	Snapshot	Ship	2008	Yang et al. (2019) ⁶	WOCE Line P18
Pacific	50.10	50.10	215.10	215.10	1.80	–	MMLD	O ₂ budget, Skin layer T correction	Full annual cycle	Float	2014–15	Yang et al. (2022) ¹²	Float No.=8397
Pacific	19.00	21.00	158.50	161.00	1.40	–	MMLD	O ₂ budget, Skin layer T correction	Full annual cycle	Float	2016–2017	Yang et al. (2022) ¹²	Float No.=9306
Pacific	-10.00	-5.00	265.00	280.00	-0.40	–	MMLD	O ₂ budget, Skin layer T correction	Full annual cycle	Float	2019–20	Yang et al. (2022) ¹²	Float No.=12775
Pacific	-2.00	2.00	190.00	270.00	1.78	0.88	MLD	DIC/DI ¹³ C budget	Snapshot	Ship	1991	Zhang and Quay (1997) ⁹²	WOCE Line P16N/US JGOFS EqPac
Pacific	-2.00	2.00	190.00	270.00	1.16	0.51	MLD	DIC/DI ¹³ C budget	Snapshot	Ship	1992	Zhang and Quay (1997) ⁹²	WOCE Line P16N/US JGOFS EqPac
Pacific	-2.00	2.00	190.00	270.00	4.19	2.30	MLD	DIC/DI ¹³ C budget	Snapshot	Ship	1992	Zhang and Quay (1997) ⁹²	WOCE Line P16N/US JGOFS EqPac

The columns of longitudes and latitudes show the longitudinal and latitudinal ranges that used for comparison with our results (boxes in [Supplementary Fig 7c](#)). Abbreviations mean the following: ANCP, annual net community production; SD, standard deviation; SE, standard error; T, temperature; MLD, mixed layer depth; MMLD, annual maximum MLD; Z_{eu}, euphotic layer depth; DIC, dissolved inorganic carbon; OUR, oxygen utilization rate; TTD, transit time distribution; TA, total alkalinity. The units for ANCP and SD/SE are mol C m⁻² year⁻¹.

Supplementary Table 2 | Methodological uncertainties in the calculations of physical oxygen fluxes

Component	Mean ± 1 SD	Source of uncertainties	
F_{ADV}	-315.6 ± 38.5	Oxygen products (2) ± 36.7	Velocity products (3) ± 10.4
F_{ADV^*}		Oxygen products (2) ± 4.5	
F_{hDIFF}	-119.6 ± 49.4	Oxygen products (2) ± 3.2	K_h products (2) ± 48.7

Numbers in parenthesis indicate the number of products that are available for the calculation.
The unit is Tmol O₂ year⁻¹.

Supplementary References

1. Gent, P. R., Willebrand, J., McDougall, T. J. & McWilliams, J. C. Parameterizing Eddy-Induced Tracer Transports in Ocean Circulation Models. *Journal of Physical Oceanography* **25**, 463–474 (1995).
2. Liang, J.-H. *et al.* Parameterizing bubble-mediated air-sea gas exchange and its effect on ocean ventilation: BUBBLE-INDUCED SUPERSATURATION. *Global Biogeochem. Cycles* **27**, 894–905 (2013).
3. Emerson, S. & Bushinsky, S. The role of bubbles during air-sea gas exchange. *J. Geophys. Res. Oceans* **121**, 4360–4376 (2016).
4. Bushinsky, S. M. & Emerson, S. Marine biological production from in situ oxygen measurements on a profiling float in the subarctic Pacific Ocean. *Global Biogeochem. Cycles* **29**, 2050–2060 (2015).
5. Plant, J. N. *et al.* Net community production at Ocean Station Papa observed with nitrate and oxygen sensors on profiling floats. *Global Biogeochem. Cycles* **30**, 859–879 (2016).
6. Yang, B., Emerson, S. R. & Quay, P. D. The Subtropical Ocean’s Biological Carbon Pump Determined From O₂ and DIC/DI¹³C Tracers. *Geophysical Research Letters* **46**, 5361–5368 (2019).
7. Yang, B., Emerson, S. R. & Bushinsky, S. M. Annual net community production in the subtropical Pacific Ocean from in situ oxygen measurements on profiling floats. *Global Biogeochemical Cycles* **31**, 728–744 (2017).
8. Emerson, S., Yang, B., White, M. & Cronin, M. Air-Sea Gas Transfer: Determining Bubble Fluxes With In Situ N₂ Observations. *J. Geophys. Res. Oceans* **124**, 2716–2727 (2019).
9. Garcia, H. E. & Gordon, L. I. Oxygen solubility in seawater: Better fitting equations. *Limnology and Oceanography* **37**, 1307–1312 (1992).
10. Large, W. G. & Pond, S. Open Ocean Momentum Flux Measurements in Moderate to Strong Winds. *Journal of Physical Oceanography* **11**, 324–336 (1981).
11. Sullivan, P. P., Romero, L., McWilliams, J. C. & Melville, W. K. Transient Evolution of Langmuir Turbulence in Ocean Boundary Layers Driven by Hurricane Winds and Waves. *Journal of Physical Oceanography* **42**, 1959–1980 (2012).
12. Yang, B., Emerson, S. R. & Cronin, M. F. Skin Temperature Correction for Calculations of Air-Sea Oxygen Flux and Annual Net Community Production. *Geophysical Research Letters* **49**, e2021GL096103 (2022).
13. Hersbach, H. *et al.* The ERA5 global reanalysis. *Quarterly Journal of the Royal Meteorological Society* **146**, 1999–2049 (2020).
14. Emerson, S. R. & Hamme, R. C. *Chemical Oceanography: Element Fluxes in the Sea*. (Cambridge University Press, 2022). doi:10.1017/9781316841174.
15. Mears, C. A. *et al.* A Near-Real-Time Version of the Cross-Calibrated Multiplatform (CCMP) Ocean Surface Wind Velocity Data Set. *JGR Oceans* **124**, 6997–7010 (2019).
16. Kobayashi, S. *et al.* The JRA-55 Reanalysis: General Specifications and Basic Characteristics. *Journal of the Meteorological Society of Japan* **93**, 5–48 (2015).
17. Gelaro, R. *et al.* The Modern-Era Retrospective Analysis for Research and Applications, Version 2 (MERRA-2). *Journal of Climate* **30**, 5419–5454 (2017).
18. DiGirolamo, N. E., Parkinson, C. L., Cavalieri, D. J., Gloersen, P. & Zwally, H. J. Sea Ice Concentrations from Nimbus-7 SMMR and DMSP SSM/I-SSMIS Passive Microwave Data. NASA National Snow and Ice Data Center Distributed Active Archive Center <https://doi.org/10.5067/MPYG15WAA4WX> (2022).

19. Schmidtko, S., Stramma, L. & Visbeck, M. Decline in global oceanic oxygen content during the past five decades. *Nature* **542**, 335–339 (2017).
20. Ito, T., Minobe, S., Long, M. C. & Deutsch, C. Upper ocean O₂ trends: 1958–2015. *Geophys. Res. Lett.* **44**, 4214–4223 (2017).
21. Helm, K. P., Bindoff, N. L. & Church, J. A. Observed decreases in oxygen content of the global ocean. *Geophys. Res. Lett.* **38**, 23602 (2011).
22. Plattner, G.-K., Joos, F. & Stocker, T. F. Revision of the global carbon budget due to changing air-sea oxygen fluxes. *Global Biogeochemical Cycles* **16**, 43-1-43-12 (2002).
23. Manning, A. C. & Keeling, R. F. Global oceanic and land biotic carbon sinks from the Scripps atmospheric oxygen flask sampling network. **58**, 95 (2006).
24. Keeling, R. F. & Manning, A. C. 5.15 - Studies of Recent Changes in Atmospheric O₂ Content. in *Treatise on Geochemistry (Second Edition)* (eds. Holland, H. D. & Turekian, K. K.) 385–404 (Elsevier, Oxford, 2014). doi:10.1016/B978-0-08-095975-7.00420-4.
25. Tohjima, Y., Mukai, H., Machida, T., Hoshina, Y. & Nakaoka, S.-I. Global carbon budgets estimated from atmospheric O₂N₂ and CO₂ observations in the western Pacific region over a 15-year period. *Atmospheric Chemistry and Physics* **19**, 9269–9285 (2019).
26. Li, C. *et al.* Estimation of Oceanic and Land Carbon Sinks Based on the Most Recent Oxygen Budget. *Earth's Future* **9**, e2021EF002124 (2021).
27. Gruber, N., Gloor, M., Fan, S.-M. & Sarmiento, J. L. Air-sea flux of oxygen estimated from bulk data: Implications For the marine and atmospheric oxygen cycles. *Global Biogeochemical Cycles* **15**, 783–803 (2001).
28. Bushinsky, S. M., Gray, A. R., Johnson, K. S. & Sarmiento, J. L. Oxygen in the Southern Ocean From Argo Floats: Determination of Processes Driving Air-Sea Fluxes. *J. Geophys. Res. Oceans* **122**, 8661–8682 (2017).
29. Li, C. *et al.* Increasing Escape of Oxygen From Oceans Under Climate Change. *Geophysical Research Letters* **47**, e2019GL086345 (2020).
30. Resplandy, L., Séferian, R. & Bopp, L. Natural variability of CO₂ and O₂ fluxes: What can we learn from centuries-long climate models simulations? *Journal of Geophysical Research: Oceans* **120**, 384–404 (2015).
31. Quay, P. Organic Matter Export Rates and the Pathways of Nutrient Supply in the Ocean. *Global Biogeochemical Cycles* **37**, e2023GB007855 (2023).
32. Watson, A. J. *et al.* Revised estimates of ocean-atmosphere CO₂ flux are consistent with ocean carbon inventory. *Nat Commun* **11**, 4422 (2020).
33. Palevsky, H. I. & Doney, S. C. How Choice of Depth Horizon Influences the Estimated Spatial Patterns and Global Magnitude of Ocean Carbon Export Flux. *Geophysical Research Letters* **45**, 4171–4179 (2018).
34. Emerson, S. & Yang, B. The Ocean's Biological Pump: In Situ Oxygen Measurements in the Subtropical Oceans. *Geophysical Research Letters* **49**, e2022GL099834 (2022).
35. Whalen, C. B., MacKinnon, J. A. & Talley, L. D. Large-scale impacts of the mesoscale environment on mixing from wind-driven internal waves. *Nature Geosci* **11**, 842–847 (2018).
36. Kouketsu, S. Inverse estimation of diffusivity coefficients from salinity distributions on isopycnal surfaces using Argo float array data. *J Oceanogr* **77**, 615–630 (2021).
37. de Lavergne, C. *et al.* A Parameterization of Local and Remote Tidal Mixing. *Journal of Advances in Modeling Earth Systems* **12**, e2020MS002065 (2020).
38. Binetti, U. *et al.* Net community oxygen production derived from Seaglider deployments at the Porcupine Abyssal Plain site (PAP; northeast Atlantic) in 2012–13. *Progress in Oceanography* **183**, 102293 (2020).

39. Brix, H., Gruber, N., Karl, D. M. & Bates, N. R. On the relationships between primary, net community, and export production in subtropical gyres. *Deep Sea Research Part II: Topical Studies in Oceanography* **53**, 698–717 (2006).
40. Gruber, N. & Keeling, C. D. *Seasonal Carbon Cycling in the Sargasso Sea near Bermuda*. (University of California Press, Berkeley, 1999).
41. Gruber, N., Keeling, C. D. & Stocker, T. F. Carbon-13 constraints on the seasonal inorganic carbon budget at the BATS site in the northwestern Sargasso Sea. *Deep Sea Research Part I: Oceanographic Research Papers* **45**, 673–717 (1998).
42. Gruber, N., Keeling, C. D. & Bates, N. R. Interannual Variability in the North Atlantic Ocean Carbon Sink. *Science* **298**, 2374–2378 (2002).
43. Hennon, T. D., Riser, S. C. & Mecking, S. Profiling float-based observations of net respiration beneath the mixed layer. *Global Biogeochemical Cycles* **30**, 920–932 (2016).
44. Jenkins, W. J. & Goldman, J. C. Seasonal oxygen cycling and primary production in the Sargasso Sea. *J Mar Res* **43**, 465–491 (1985).
45. Johnson, K. S., Plant, J. N., Dunne, J. P., Talley, L. D. & Sarmiento, J. L. Annual nitrate drawdown observed by SOCCOM profiling floats and the relationship to annual net community production. *Journal of Geophysical Research: Oceans* **122**, 6668–6683 (2017).
46. Munro, D. R. *et al.* Estimates of net community production in the Southern Ocean determined from time series observations (2002–2011) of nutrients, dissolved inorganic carbon, and surface ocean pCO₂ in Drake Passage. *Deep Sea Research Part II: Topical Studies in Oceanography* **114**, 49–63 (2015).
47. Neuer, S. *et al.* Biogeochemistry and hydrography in the eastern subtropical North Atlantic gyre. Results from the European time-series station ESTOC. *Progress in Oceanography* **72**, 1–29 (2007).
48. Quay, P., Stutsman, J. & Steinhoff, T. Primary production and carbon export rates across the subpolar N. Atlantic Ocean basin based on triple oxygen isotope and dissolved O₂ and Ar gas measurements. *Global Biogeochemical Cycles* **26**, (2012).
49. Quay, P., Emerson, S. & Palevsky, H. Regional Pattern of the Ocean's Biological Pump Based on Geochemical Observations. *Geophys. Res. Lett.* **47**, (2020).
50. Spitzer, W. S. & Jenkins, W. J. Rates of vertical mixing, gas exchange and new production: Estimates from seasonal gas cycles in the upper ocean near Bermuda. *J Mar Res* **47**, 169–196 (1989).
51. Stanley, R. H. R., Doney, S. C., Jenkins, W. J. & Lott, I. I. I. Apparent oxygen utilization rates calculated from tritium and helium-3 profiles at the Bermuda Atlantic Time-series Study site. *Biogeosciences* **9**, 1969–1983 (2012).
52. Stanley, R. H. R., Jenkins, W. J., Doney, S. C. & Lott III, D. E. The ³He flux gauge in the Sargasso Sea: a determination of physical nutrient fluxes to the euphotic zone at the Bermuda Atlantic Time-series Site. *Biogeosciences* **12**, 5199–5210 (2015).
53. Arteaga, L. A., Pahlow, M., Bushinsky, S. M. & Sarmiento, J. L. Nutrient Controls on Export Production in the Southern Ocean. *Global Biogeochem. Cycles* **33**, 942–956 (2019).
54. MacCready, P. & Quay, P. Biological export flux in the Southern Ocean estimated from a climatological nitrate budget. *Deep Sea Research Part II: Topical Studies in Oceanography* **48**, 4299–4322 (2001).
55. Benitez-Nelson, C., Buesseler, K. O., Karl, D. M. & Andrews, J. A time-series study of particulate matter export in the North Pacific Subtropical Gyre based on ²³⁴Th:²³⁸U disequilibrium. *Deep Sea Research Part I: Oceanographic Research Papers* **48**, 2595–2611 (2001).

56. Brix, H., Gruber, N. & Keeling, C. D. Interannual variability of the upper ocean carbon cycle at station ALOHA near Hawaii. *Global Biogeochemical Cycles* **18**, (2004).
57. Emerson, S. Seasonal oxygen cycles and biological new production in surface waters of the subarctic Pacific Ocean. *Journal of Geophysical Research: Oceans* **92**, 6535–6544 (1987).
58. Emerson, S. & Stump, C. Net biological oxygen production in the ocean—II: Remote in situ measurements of O₂ and N₂ in subarctic pacific surface waters. *Deep Sea Research Part I: Oceanographic Research Papers* **57**, 1255–1265 (2010).
59. Emerson, S., Quay, P., Stump, C., Wilbur, D. & Knox, M. O₂, Ar, N₂, and 222Rn in surface waters of the subarctic Ocean: Net biological O₂ production. *Global Biogeochemical Cycles* **5**, 49–69 (1991).
60. Emerson, S., Quay, P. D., Stump, C., Wilbur, D. & Schudlich, R. Chemical tracers of productivity and respiration in the subtropical Pacific Ocean. *Journal of Geophysical Research: Oceans* **100**, 15873–15887 (1995).
61. Emerson, S. *et al.* Experimental determination of the organic carbon flux from open-ocean surface waters. *Nature* **389**, 951–954 (1997).
62. Emerson, S., Stump, C. & Nicholson, D. Net biological oxygen production in the ocean: Remote in situ measurements of O₂ and N₂ in surface waters. *Global Biogeochemical Cycles* **22**, (2008).
63. Fassbender, A. J., Sabine, C. L. & Cronin, M. F. Net community production and calcification from 7 years of NOAA Station Papa Mooring measurements. *Global Biogeochemical Cycles* **30**, 250–267 (2016).
64. Fassbender, A. J., Sabine, C. L., Cronin, M. F. & Sutton, A. J. Mixed-layer carbon cycling at the Kuroshio Extension Observatory. *Global Biogeochemical Cycles* **31**, 272–288 (2017).
65. Ferrón, S., Barone, B., Church, M. J., White, A. E. & Karl, D. M. Euphotic Zone Metabolism in the North Pacific Subtropical Gyre Based on Oxygen Dynamics. *Global Biogeochemical Cycles* **35**, e2020GB006744 (2021).
66. Hamme, R. C. & Emerson, S. R. Constraining bubble dynamics and mixing with dissolved gases: Implications for productivity measurements by oxygen mass balance. *J Mar Res* **64**, 73–95 (2006).
67. Hashihama, F. *et al.* Nanomolar phosphate supply and its recycling drive net community production in the subtropical North Pacific. *Nat Commun* **12**, 3462 (2021).
68. Haskell, W. Z., Fassbender, A. J., Long, J. S. & Plant, J. N. Annual Net Community Production of Particulate and Dissolved Organic Carbon From a Decade of Biogeochemical Profiling Float Observations in the Northeast Pacific. *Global Biogeochem. Cycles* **34**, (2020).
69. Hendricks, M. B., Bender, M. L., Barnett, B. A., Strutton, P. & Chavez, F. P. Triple oxygen isotope composition of dissolved O₂ in the equatorial Pacific: A tracer of mixing, production, and respiration. *Journal of Geophysical Research: Oceans* **110**, (2005).
70. Huang, Y., Fassbender, A. J., Long, J. S., Johannessen, S. & Bernardi Bif, M. Partitioning the Export of Distinct Biogenic Carbon Pools in the Northeast Pacific Ocean Using a Biogeochemical Profiling Float. *Global Biogeochemical Cycles* **36**, e2021GB007178 (2022).
71. Ishii, M. *et al.* Seasonal variation in total inorganic carbon and its controlling processes in surface waters of the western North Pacific subtropical gyre. *Marine Chemistry* **75**, 17–32 (2001).
72. Jenkins, W. J. & Doney, S. C. The subtropical nutrient spiral. *Global Biogeochemical Cycles* **17**, (2003).

73. Kaiser, J., Reuer, M. K., Barnett, B. & Bender, M. L. Marine productivity estimates from continuous O₂/Ar ratio measurements by membrane inlet mass spectrometry. *Geophysical Research Letters* **32**, (2005).
74. Keeling, C. D., Brix, H. & Gruber, N. Seasonal and long-term dynamics of the upper ocean carbon cycle at Station ALOHA near Hawaii. *Global Biogeochemical Cycles* **18**, (2004).
75. Knor, L. A. C. M. *et al.* Quantifying Net Community Production and Calcification at Station ALOHA Near Hawai'i: Insights and Limitations From a Dual Tracer Carbon Budget Approach. *Global Biogeochemical Cycles* **37**, e2022GB007672 (2023).
76. Martz, T. R., Johnson, K. S. & Riser, S. C. Ocean metabolism observed with oxygen sensors on profiling floats in the South Pacific. *Limnology and Oceanography* **53**, 2094–2111 (2008).
77. Midorikawa, T. *et al.* Estimation of seasonal net community production and air-sea CO₂ flux based on the carbon budget above the temperature minimum layer in the western subarctic North Pacific. *Deep Sea Research Part I: Oceanographic Research Papers* **49**, 339–362 (2002).
78. Munro, D. R., Quay, P. D., Juranek, L. W. & Goericke, R. Biological production rates off the Southern California coast estimated from triple O₂ isotopes and O₂ : Ar gas ratios. *Limnology and Oceanography* **58**, 1312–1328 (2013).
79. Palevsky, H. I., Quay, P. D., Lockwood, D. E. & Nicholson, D. P. The annual cycle of gross primary production, net community production, and export efficiency across the North Pacific Ocean. *Global Biogeochemical Cycles* **30**, 361–380 (2016).
80. Pelland, N. A., Eriksen, C. C., Emerson, S. R. & Cronin, M. F. Seaglider Surveys at Ocean Station Papa: Oxygen Kinematics and Upper-Ocean Metabolism. *Journal of Geophysical Research: Oceans* **123**, 6408–6427 (2018).
81. Quay, P. & Stutsman, J. Surface layer carbon budget for the subtropical N. Pacific: δ¹³C constraints at station ALOHA. *Deep Sea Research Part I: Oceanographic Research Papers* **50**, 1045–1061 (2003).
82. Quay, P. D., Stutsman, J., Feely, R. A. & Juranek, L. W. Net community production rates across the subtropical and equatorial Pacific Ocean estimated from air-sea δ¹³C disequilibrium. *Global Biogeochemical Cycles* **23**, (2009).
83. Quay, P. D., Peacock, C., Björkman, K. & Karl, D. M. Measuring primary production rates in the ocean: Enigmatic results between incubation and non-incubation methods at Station ALOHA. *Global Biogeochemical Cycles* **24**, (2010).
84. Riser, S. C. & Johnson, K. S. Net production of oxygen in the subtropical ocean. *Nature* **451**, 323–325 (2008).
85. Shadwick, E. H. *et al.* Seasonality of biological and physical controls on surface ocean CO₂ from hourly observations at the Southern Ocean Time Series site south of Australia. *Global Biogeochemical Cycles* **29**, 223–238 (2015).
86. Sonnerup, R. E., Mecking, S. & Bullister, J. L. Transit time distributions and oxygen utilization rates in the Northeast Pacific Ocean from chlorofluorocarbons and sulfur hexafluoride. *Deep Sea Research Part I: Oceanographic Research Papers* **72**, 61–71 (2013).
87. Sonnerup, R. E., Mecking, S., Bullister, J. L. & Warner, M. J. Transit time distributions and oxygen utilization rates from chlorofluorocarbons and sulfur hexafluoride in the Southeast Pacific Ocean. *Journal of Geophysical Research: Oceans* **120**, 3761–3776 (2015).
88. Stanley, R. H. R., Kirkpatrick, J. B., Cassar, N., Barnett, B. A. & Bender, M. L. Net community production and gross primary production rates in the western equatorial Pacific. *Global Biogeochemical Cycles* **24**, (2010).

89. Wakita, M. *et al.* Biological organic carbon export estimated from the annual carbon budget observed in the surface waters of the western subarctic and subtropical North Pacific Ocean from 2004 to 2013. *J Oceanogr* **72**, 665–685 (2016).
90. Wong, C. S. *et al.* Seasonal cycles of nutrients and dissolved inorganic carbon at high and mid latitudes in the North Pacific Ocean during the Skaugran cruises: determination of new production and nutrient uptake ratios. *Deep Sea Research Part II: Topical Studies in Oceanography* **49**, 5317–5338 (2002).
91. Yang, B., Emerson, S. R. & Peña, M. A. The effect of the 2013–2016 high temperature anomaly in the subarctic Northeast Pacific (the “Blob”) on net community production. *Biogeosciences* **15**, 6747–6759 (2018).
92. Zhang, J. & Quay, P. D. The total organic carbon export rate based on ^{13}C and ^{12}C of DIC budgets in the equatorial Pacific region. *Deep Sea Research Part II: Topical Studies in Oceanography* **44**, 2163–2190 (1997).